



**University of Kerbala
College of Science
Department of Chemistry**

***Design and Investigation of New Hybrid Materials as
Nonlinear Optical Chromophores***

A Thesis Submitted to the Council of the College of Science,
University of Kerbala in Partial Fulfilment of the Requirements for the
Master Degree Science of Chemistry

Written By

Khamis Shalal Ghayad

Supervised by

Prof. Dr.

Ahmed Hadi AlYasari

Muharram 1447 AH

Asst. Prof. Dr.

Thaer Mahdi Madlool

July 2025 A.D

بِسْمِ اللَّهِ الرَّحْمَنِ الرَّحِيمِ

﴿نرفع درجات من نشاء وفوق كل ذي علم عليم﴾

صدق الله العلي العظيم

سورة يوسف جزء من الآية (76) ﴿

Dedication

To the one who turned adversity into a grant.. Allah....

To the savior of the world's injustice... Imam Mehdi (May

Allah hasten his relief)...

To the holy blood... The martyrs of Iraq ..

To the angels in my life... The soul of my father and mother

To the roses blooming in the hardest days... our Children.

To those who encourage me and helped me thro ughout my

scholarly journey the length of our life ...

my teachers and our friends.

Dedicate this work with love and gratitude.

Khamis

Acknowledgments

Praise be to God for the blessings bestowed upon me, I extend my deepest thanks and gratitude my supervisors to Prof. Dr. **Ahmed Hadi AlYasari**, who kindly accepted the supervision of my master's thesis and gave me his valuable time and whose extensive experience formed a great addition to the research work.

I would like to extend my gratitude to Assistant Professor Dr. **Thaer Mahdi Al-Ramahi** who stood by me during the period of preparatory and research study. His valuable guidance and patience during the period of his assumption of the position of head of the department, advice were the guidnglight that I throughout my research work.

I would like thank the respected Dean of the Faculty of Science and the respected Head of the Department of Chemistry for their honorable stand with me during the research period and their continuous inspection of the progress of my research work...

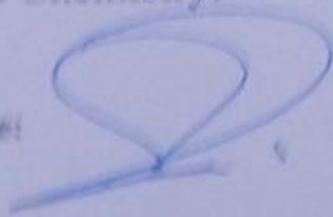
I express my thanks to the people of my house, my dear wife and children who are the fruit of my heart, and the best support throughout the days of my life ...

I would also like to thank my dear brother and friend, Mr. **Mohammed Hassan Al-Battat**, for his continuous and uninterrupted support throughout the preparatory and research study period. I also extend my sincere thanks to the faculty members and colleagues who helped me at the University of Karbala /College of Science /Department of Chemistry. Finally, I would also like to thank all the members of the screening committee for accepting the master's thesis discussion.

Supervisor Certification

I hereby certify that this thesis, entitled (**Design and Study of New Hybrid Materials as Nonlinear Optical Chromophores**), has been prepared by the student "**Khamis Shalal Ghayad**" under my supervision in the Department of Chemistry, College of Science, University of Kerbala, as a partial requirement for the Master's degree in Chemistry.

Signature:



Name: **Dr. Ahmed Hadi Abdul Amir**

Title: **Professor.**

Address: **University of Kerbala, College of Applied Medical Sciences**

Date: **23 / 7 / 2025**

Signature:



Name: **Dr. Thaer Mahdi Madloul**

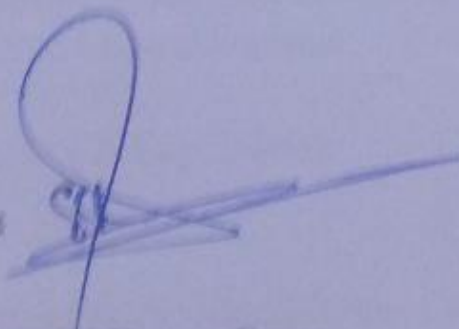
Title: **Assistant. Professor.**

Address: **University of Kerbala, College of Sciences , Department of Chemistry**

Date: **23 / 7 / 2025**

In View of the available recommendations by the Supervisor, I forward this thesis for debate by the examining committee.

Signature:



Name: **Dr. Sajid Hassan Guzar**

Title: **Professor.**

Head of Chemistry Department /College of Science,

Date: **/ / 2025**

Examination Committee Certification

We certify that we have read this thesis entitled "*Design and Investigation of New Hybrid Materials as Nonlinear Optical Chromophores*" As the examining committee, examined the student "*Khamis Shalal Ghayad*" on its contents, and that in our opinion; it is adequate for the partial fulfillment of the requirements for the Degree of Master in Science of Chemistry,

Signature: 

Name: **Dr. Hamida Eidan Salman**

Title: Professor

Address: University of Karbala / College of Education for Pure Sciences

Date: / /2025

(Chairman)

Signature: 


Name: **Dr. Haider Abdul Razzaq Abdul Hussein**

Title: Assistance Professor

Address: University of Kufa / College of Science.

Date: 9 / 9 /2025

(Member)

Signature: 


Name: **Dr. Ahmed Hadi Abdul Amir**

Title: Professor

Address: University of Kerbala, College of, Applied Medical Sciences.

Date: 23 / 7 /2025

(Member & Supervisor)

Signature: 

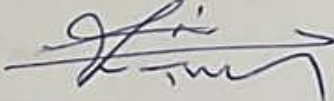
Name: **Dr. Manal Abd Mohamed Toofan**

Title: Assistance Professor

Address: University of Karbala / College of Science. Department of Chemistry.

Date: 8 / 9 /2025

(Member)

Signature: 

Name: **Dr. Thaer Mahdi Madloul**


Title: Assistance Professor

Address: University of Kerbala, College of Science, Department of Chemistry.

Date: / /2025

(Member & Supervisor)

Approved by the council of the College of Science

Signature: 

Name: **Dr. Hassan Jameel Jawad ALfatlawy**

Title: Professor

Address: Dean of College of Science, University of Kerbala.

Date: / /2025

Abstract

Three sections make up this thesis. An introduction to non-linear optical (NLO) materials and second-harmonic Generation (SHG) formation is covered in the first section, along with an explanation of the donor-acceptor relationship and how bridges are used in the Two-State Model to connect them. Additionally Polyoxometalate (POM) and its variants, are discussed as well as pyrene, the strongest donor known. The second section examines the Schrödinger equation, includes four key approximations, quantum chemistry, and Hartree-Fock (HF). It also TDDFT, DFT, and other related subjects. All of the results were described in the third part. Through second-order phenomena like second harmonic production (frequency doubling) and third-order effects like multi-photon absorption, non-linear optical (NLO) materials are utilized to alter laser light. This thesis focuses on NLO materials that include phenyl-imido groups that link organic electron donors to polyoxometalate (POM) electron acceptors. We have thoroughly investigated novel compounds as strong NLO chemicals, such as pyrene-based donor groups, which are incredibly powerful donors, both theoretically and mostly by DFT calculations. Additionally, their linear optical properties, second-order nonlinear responses, and geometric and electrical structures have all been assessed. Moreover, the effects of substitutions (such alkyl and phenyl groups) on the donor strength of pyrene and, therefore, on the responses have been investigated. Anion 5 produced a remarkable NLO responses of up to $(1349 \times 10^{-30} \text{esu})$ an increase of ≈ 2 compared to its un-methylated analogue (anion 2). TD-DFT calculations indicate that the strong low-energy transition is mainly caused by the charge transfer (CT) from pyrene arylamide to the hexamolybdate cluster. According to this, the compounds' linear and non-linear optical behaviour is caused by substantial communication between the POM and pyrene

components. Even though it drastically lessens the initial hyperpolarizability, ortho-methylation of the imido-bond has a considerable impact on the stability and, consequently, the length and linearity of the bond as well as the NLO activity. While maintaining a respectably high transparency window, the TDDFT results show that the pyrene-POMs combination exhibits extraordinary NLO activity in comparison to similar simple organic systems.

Subjects		
Subject		Page
Abstract		I.
		II.
List of Tables		III.
List of Figures		IV.
List of Schemes		V.
List of abbreviations and Symbols		VI.
List of costents		VII.
List of Tables		
No.	Subject	Page
1.1	Advantages AND Disadvantages OF Inorganic and organic materials	8-9
1.2	First Hyperpolarizabilities (β) of selected molecular chromophores' in (10^{-30}) <i>esu</i>	11
2.1	A chronology of quantum research turning points that established the area of quantum biology	36
3.1	Selected structural constants for the geometries of compounds 1, 2, 3, 5, and 6 with distances in (Å) and angles in (°).	54
3.2	Calculated Initial Hyperpolarizabilities ($\times 10^{-30}$ <i>esu</i>) Of Anions 1-6 compared With predicted and experimental Values For compound DAST	57
3.3	The electronic transition energy (E_{\max}), oscillator strength (f_{os}), maximum absorption wavelength (λ_{\max}), and the % Mo contribution were computed.	62

List of Figures

No.	Subject	Page
1.1	Illustration of the Process of Induced Polarization, which Doubles the frequency of Incoming Light	3
1.2	Two-photon excited fluorescence versus SHG. Displayed are the Perrin–Jablonski fluorescence diagram (Left) and the energy-level diagram (Right) describing two-photon excited fluorescence and SHG, respectively	4
1.3	Represent structures of conventional push-pull NLO active chromophores	9
1.4	Common structures of polyoxometalates: Bull- and – stick and polyhedral Representations of the three most prevalent polyoxometalate anions :(a)anion (Lindqvist)[Mo ₆ O ₁₉] ⁿ⁻ (b){ α -{XO ₄ }M ₁₂ O ₃₆ } (c)[α {XO ₄ } ₂ M ₈ O ₅₄] γ -keggin anion γ -wells -Dawson configuration	21
2.1	Interdisciplinary Foundations of quantum chemistry	30
2.2	Catalysis by Enzymes Via Quantum Tunneling	37
2.3	Slater and Gaussian Functions or an orbital of size 1s. The Slater function is a good illustration of a hydrogen atom because of its sharp point at the apex. The photograph was taken by Moradabadi, A. While SCM-ADF employs STOs, Gaussian code often uses Gaussian type functions.	48
2.4	creation of a pseudo-Slater function is produced by combining Gaussian type functions.	48
2.5	Diagram explaining differences between High Throughput and Inverse Design development methods	51
3.1	Solvent-Phase Optimized Geometries anions 1–6. Red O, Blue = N, white = H, Cyan = Mo, and Gray = C.	55
3.2	TD-DFT-Calculated UV-Vis Spectra for NO. (1, 2, 3, 4,5 and 6) Accordingly	61
3.3	The Molecular Orbitals involved in Significant Transitions of HOMO and LUMO No.1.	63
3.4	The Molecular Orbitals involved in Significant Transitions of HOMO and LUMO No. 2.	64
3.5	The Molecular Orbitals involved in Significant Transitions of HOMO and LUMO No.3.	65

3.6	The Molecular Orbitals involved in Significant Transitions of HOMO and LUMO No. 4.	66
3.7	The Molecular Orbitals involved in Significant Transitions of HOMO and LUMO NO. 5	67
List of schemes		
No.	Subject	Page
1.1	Sylate-forming Structure of Dimethylamino-N-Methyl-4-Stilbazolium (DAST)	15
1.2	Structural Representation of Linkers Enabling Electron Communication Between POMs and Pyrene Units in Hybrid Materials	27
3.1	Molecular Structures of hexamolybdate-organoimido-pyrene compounds 1-6	53

List of Abbreviations	
Symbol	Definition
A	Acceptor
BS	Basis Sets
CC	Coupled Cluster
CI	Configuration Interaction
CT	Charge -Transfer
D	Donor
DAST	Dimethyl - Amino -Stilbazolium Tosylate
AO	Atomic Orbital
DFT	Density Functional Theory
EFISH	Electric Field Induced Second Harmonic Generation
DH	Double Hybrid
SH	second-harmonic

LASER	Light Amplication by Stimulated Emission of Radiation
UV	Ultra-Violet
α	linearly
ϵ_0	permittivity of empty space
E	Field electrical
EESs	Electrical Energy Storages
E_{\max}	Energy transfer between the ground and excited states in optics
P	polarization
P_L	Polarization linear
P_{NL}	Polarization nonlinear
EO	Electro - Optical
FMs	Function Modules
GGA	Generalized Gradient Approximation
GTO	Gaussian Type Orbital
HF	Hartree - Fock
HOMO	High Energy Occupied Molecular Orbitals
HRS	Hyper - Raleigh Scattering
ICT	Intramolecular Charge - Transfer
THG	third-harmonic generation
TPA	two-photon absorption
ICTL	Intramolecular Charge Transfer Layers
LC	Long - Range Corrected
LUMO	Low Energy Unoccupied Molecular Orbitals
MBPT	Many - Body perturbation Theory
NLO	Non - Linear Optical
POH	Plasmonic-organic hybrid
OR	Optical Rectification

POMs	Polyoxometalates
QC	Quantum Chemistry
QZ	Quadruple Zeta
RS	Range Separated
SFG	Sum Frequency Generation
SHG	second-harmonic Generation
STOs	Slater Type Orbitals
TDDFT	Time - Dependent Density Functional Theory
THz	Terahertz
C_n	Coefficient number
ECP	Effective core potentials
DCT	Distance of charge transfer
DCC	N,N-Di cyclohexyl carbodiimide
DMSO	Dimethyl sulfoxide
H ₂ O	water
ζ	Orbital exponent
\hat{T}	Kinetic Energy Operator
∇^2	Laplacian Operator
\hat{H}	Hamiltonian operator
Ψ	Wave Function
β	Second - order polarizability or (the first hyperpolarizability)
F_{os}	Oscillator strength
β^o	First hyperpolarizability
$\Delta \mu_{12}$	Dipole Moment Change
$\mu_{1,2}$	Dipole Moment
E_{MAX}	Electronic transition energy
λ_{max}	Wavelength at maximum absorption

χ^2	Second-Order Nonlinear Susceptibility	
χ^3	Third-Order Nonlinear Susceptibility	
ω_1, ω_2	Optical frequency	
List of contents		
No.	Subject	page
$\Psi(r, \theta, \varphi)$	complete description of 3-D electron wavefunction	34
$R_{n,l}(r)$	radial component (z-axis contribution)	34
$Y(\theta, \varphi)$	$(\cos\theta) e^{im\varphi}$ = angular component (x- and y-axis contribution)	34
N	total collection of constants	34
n	principal quantum number (1, 2, ...)	34
l	azimuthal quantum number (0, 1, 2, ..., n-1)	34
m	magnetic quantum number (-n-1, ... -2, -1, 0, 1, 2, n-1)	34
h	Planck constant = $6.626 \times 10^{-34} JS$	35
E[P]	Electron Density	42
TS[p]	Kinetic Energy	42
$v_{ext}(r)$	the ions are “external” to the N-electron system	42
Chapter One		
Introduction		
No.	Subject	page
1.1	Background	1
1.2	Foundational Ideas	1
1.3	A Historical View on Nonlinear Optics	3
1.4	Key Nonlinear Optical Phenomena	4
1.4.1	Second-Harmonic Generation (SHG)	4

1.4.2	Third-Harmonic Generation (THG)	4
1.4.3	Two-Photon Absorption (TPA)	4
1.4.4	Self-Focusing and Self-Phase Modulation	4
1.5	Two States Model	5
1.6	Application of second Harmonic Generation (SHG)	5
1.7	Methods for Measuring First Hyperpolarizability Experimentally (β)	6
1.7.1	Electric Field-Induced Second Harmonic Generation(EFISH)	6
1.7.2	Hyper-Rayleigh Scattering (HRS):	7
1.8	NLO Materials	7
1.9	A Comparitue Analysis of Organic and Inorganic compounds	8
1.9.1	Organic/Metallo-organic based NLO Materials	11
1.10	Chromophores D- π -A	17
1.11	Changeable NLO	18
1.12	Polyoxometalates (POMs)	19
1.12.1	Derivatives of Lindqvist-Organoimido	21
1.12.2	Literature survey On Organoimido-Lindqvist as NLO Materials	24
1.13	Pyrene-based Donors	26
1.14	Aims of Study	28

Chapter TWO		
Computational Theory and Method		
No.	Subject	Page
2.1	Computational Chemistry	29
2.2	History and Software of Computational Chemistry	29
2.3	Methods of Computation	31
2.3.1	Hyperpolarizability and the Analysis of Two-State Models	32
2.4	Quantum Mechanics	33
2.5	Quantum biology	35
2.5.1	Important Turning Points in Quantum Research	36
2.5.2	mathematical and physical Formation sol Quantum biology's underpinnings	37
2.6	Schrödinger Equation	37
2.7	Hartree-Fock Self Consistent Field	40
2.8	Electron Correlation	41
2.9	Density Functional Theory (DFT)	41
2.9.1	Time-Dependent Density Functional Theory (TD-DFT)	44
2.9.2	ω B97XD	46
2.10	Basis Sets	46
2.10.1	LANL2TZ	50
2.11	Inverse Design	50

Chapter Three
Results and Discussion

No.	Subject	page
3.1	Results and Discussions	53
3.2	Molecular Geometries in the Ground State for 1–6 Compounds	54
3.3	Properties Of NLO: Initial Hyperpolarizabilities For 1–6 Substances	56
3.4	The UV-visible absorption spectra of compounds 1–6	57
3.5	Conclusion	68
3.6	Future Projects	69

References

CHAPTER ONE

INTRODUCTION

INTRODUCTION

1.1 Background:

Nonlinear optics (NLO) is a branch of optics that examines the behavior of light. In nonlinear media, a material's reaction to an electromagnetic field is not exactly proportional to the field's intensity^[1] When Laser was developed, it gave rise to this discipline in the early 1960s since it offered the powerful light sources required to examine nonlinear optical processes^[2] In contrast to linear optics, which uses the superposition principle, nonlinear optics incorporates interactions that can produce new frequencies, alter the way light propagates, and produce a host of other intricate effects^[3].

1.2 Foundational Ideas:

The nonlinear polarization of the medium is the fundamental concept in nonlinear optics^[4]. A material subjected to a strong electromagnetic field, such as that created by a laser, may have its induced polarization (P) calculated using the following formula:

$$P = \epsilon_0 (\chi^{(1)}E + \chi^{(2)}E^2 + \chi^{(3)}E^3 + \dots) \dots \dots \dots \text{(Eq.1.1)}$$

where $\chi^{(n)}$ represents the nth-order nonlinear susceptibilities, E represents the electric field, and ϵ_0 represents the permittivity of empty space. These susceptibilities lead to nonlinear optical phenomena, such as two-photon absorption (TPA), third harmonic generation (THG), and second harmonic generation (SHG), which determine the intensity of the nonlinear response^[5]. Because of this interaction, an induced dipole moment is created that oscillates at the same frequency as the applied light field. When the incoming light intensity is relatively low, equation (1-2) shows that the electric field and the induced electric-dipole moment are linearly related (α).

$$\text{Polarization} = \mu = \alpha E \dots \dots \dots \text{(Eq.1.2)}$$

Equation 1.2 uses the linear susceptibility (χ) of a group of molecules for bulk or macroscopic materials.



$$P = \chi E \dots \dots \dots (Eq.1.3)$$

The polarization explains the material's optical characteristics, including absorption, reflection, refraction, and diffusion. At that frequency, it emits radiation and functions as A source .The induced dipole moments and the electric field no longer have a linear relationship when the electric field of the light is large, and the optical susceptibility (χ) is altered when the electric field is applied. This implies that the applied electric field's power series might be used to express the polarization^[6] .

$$P = P_L + P_{NL} \dots \dots \dots (Eq.1.4) \text{ or}$$

$$P = X^1 E + X^2 EE + X^3 EEE + \dots \dots \dots (Eq.1.5)$$

$$\mu = \alpha E + \beta EE + \gamma EEE + \dots \dots \dots (Eq.1.6)$$

where p is polarization, P_L is polarization linear, P_{NL} is polarization nonlinear, x¹ is first -order linear susceptibility, x² is second-order nonlinear susceptibility, x³ is third-order nonlinear susceptibility, E⁽ⁿ⁾ is the electric field, With a second-order non-linear susceptibility acting as a source of radiation at new frequencies, 2ω₁, 2ω₂, ω₁+ω₂, and |ω₁-ω₂|, the non-linear polarization of a material can be used to explain the onset of non-linear phenomena like SHG, sum frequency generation (SFG), difference frequency mixing (DFM), and optical rectification (OR). α represents linear polarizability, β represents second-order polarizability, and γ represents third-order polarizability or second hyperpolarizability as illustrated in Figure1. The initial hyperpolarizability, β, is a third rank tensor with 27 non-independent elements that needs symmetry. Some of these 27 components, for instance, vanish depending on the symmetry of the molecule; for centrosymmetric materials, the initial hyperpolarizability is β₀. These 27 items represent the different combinations of the three Cartesian elements of polarization and the two interacting electric fields. The main topics of this dissertation are frequency doubling and SHG. Usually, only a very tiny percentage of these 27 components are non-zero since molecular symmetry may be used to reduce them. The 27 tensors may be reduced to a single

component by ignoring the others because, for each Often, only one component of the molecule studied in this work is noticeably larger than the rest.

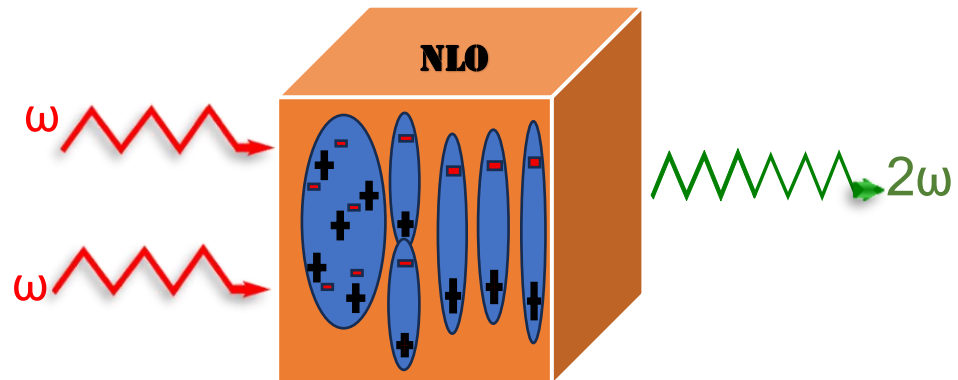


Figure 1.1 Illustration of the Process of Induced Polarization, which doubles the frequency of the Incoming Light ^[7]

1.3 A Historical View on Nonlinear Optics

The history of the field may be traced back to the late nineteenth century, when some of the nonlinear optical phenomena were being described. The area of nonlinear optics began with the publication of one of the most well-known nonlinear phenomena, the Kerr effect or optical Kerr effect, by John Kerr in 1875 ^[8]. Friedrich Pockels identified the first NLO phenomena in 1884, a few years later, and called it the Pockels effect. But in reality, the current age of nonlinear optics began in 1960 when Theodore Maiman invented the first usable laser and in 1961 when Franken used the laser to discover the phenomena known as second harmonic generation (SHG)^{[6][9]}. The development of effective laser technology paralleled the development of nonlinear optics. Numerous studies in this Field have advanced it, and numerous intriguing new nonlinear optical phenomena have been discovered. Example timeline below highlights significant findings in the field of NLO.

1.4 Key Nonlinear Optical Phenomena:

1.4.1 Second-Harmonic Generation (SHG):

Frequency doubling, or SHG, is the process by which two photons with the same frequency combine to create a new photon with twice the energy and, consequently, twice the frequency. According to Munn^[10], this phenomenon is frequently employed in laser technology to transform infrared energy into visible light^[11].

1.4.2 Third-Harmonic Generation (THG):

The interaction of three photons in THG results in a single photon with three times the frequency of SHG. THG is employed in spectroscopy and microscopy, among other fields^[12].

1.4.3 Two-Photon Absorption (TPA):

Because the combined energy of the photons stimulates an electron to a higher energy state, TPA occurs when two photons are absorbed at the same time. Two-photon microscopy uses this phenomenon to provide deeper and more accurate imaging of biological tissues.^[13]

1.4.4 Self-Focusing and Self-Phase Modulation:

High-intensity light can affect a medium's refractive index, leading to self-focusing or self-phase modulation. Laser pulse propagation is impacted by these factors^[6]

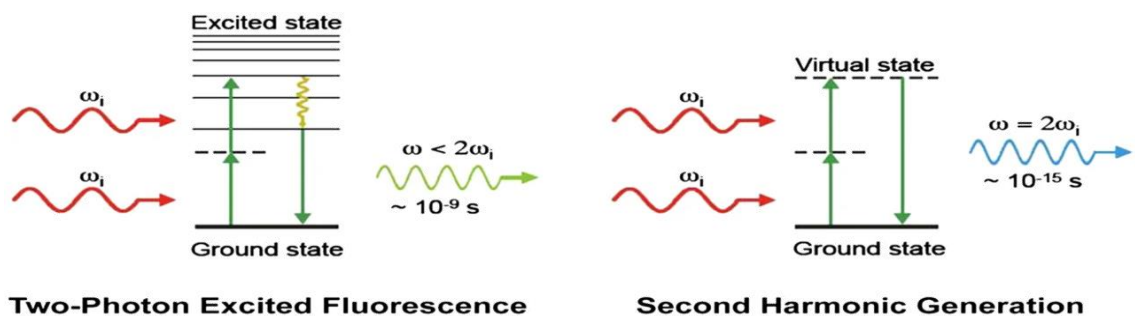


Figure 1.2 Two-photon excited fluorescence versus SHG. Displayed are the Perrin–Jablonski fluorescence diagram (Left) and the energy-level diagram (Right) describing two-photon excited fluorescence and SHG, respectively^[15]

1.5 Two States Model:

Chemla and Oudar's two-state paradigm^[14] discusses the chemical characteristics and initial hyperpolarizability that might be utilized to aid in the creation of compounds that function as NLO chromophores. Increased excited states may resonantly improve the initial hyperpolarizability if the chemical in question has an absorption band around the fundamental or second-harmonic (SH) wavelength. The static (off-resonance) initial hyperpolarizability β_0 may be used to compare the quadratic NLO quality at different wavelengths, as it is thought that the NLO qualities are produced by a single transition^[15].

$$\beta_0 = \frac{3\Delta\mu_{12}(\mu_{12})^2}{2(E_{MAX})^2} \dots\dots\dots(\text{Eq1-7})$$

where $\Delta\mu_{12}$ is the change in dipole moment between the ground and excited state, μ_{12} is the electronic transition dipole moment, and E_{max} is the optical transition energy between the ground and excited state. β is frequency dependent when measured in non-resonant circumstances without SH reabsorption, whereas β_0 , or β extrapolated to zero frequency, is by definition not. An important overestimation or underestimating might arise from the possibility of additional excited states. A reduction in the intramolecular charge-transfer energy, E_{max} , causes an increase in β_0 (ICT). A wavelength of λ is the wavelength of the incoming light (laser) in the measurement, and λ_{max} is the wavelength of maximum absorption. The second harmonic's wavelength must fall inside the off-resonant zone for this model to function.

1.6 Application of second Harmonic Generation (SHG):

A second harmonic radiation is produced via the most popular of the several uses of the SHG phenomenon, frequency doubling^[10]. In order to get coherent optical radiations with entirely different wavelengths than the currently available wavelength laser source, it is commonly utilized in laboratories for pragmatic reasons^[14]. Materials with measurable SHG

effects can be employed as electro-optic modulators to function as switching elements for signal transformations, which is another important use outside of the lab in optical-fiber communications [16]. Other application areas include study on materials interfaces, magneto-optics, and surface phenomena such as absorptions, molecule orientations, and aggregations [17].

1.7 Methods for Measuring First Hyperpolarizability

Experimentally (β)

1.7.1 Electric Field-Induced Second Harmonic Generation(EFISH):

One obtains a projected vectorial in the direction of the molecule dipole in the EFISH experiment^[4]. Applying a high electric field (static) to an NLO chromophore solution is part of the approach. In the presence of applied field and in the solution, the molecules will orient in a certain direction due to their permanent dipoles (average orientations will be more directional)^[17].

Second Harmonic Generation (SHG),The scalar product of the applied field and Molecule dipole vectors is what is obtained as a result of the experiment. The values must also be known in order to compute the precise value of (β)from the experiment^[18] [19]. These values can be found independently, and THG experiments are really required. In the event that the material exhibits significant charge transfer (CT) transitions, the contributions from these sources may be readily disregarded with reasonable accuracy because the CT transitions should be far greater. Since this experimental process employs solutions for measurements, materials are dissolved in appropriate solvents using the right techniques, making it simple to discern the contributions of the solvent and the solute. Interpreting experimental data becomes difficult when molecules do not exhibit strong, nearly unidirectional charge transport axis along the dipole directions. Additionally, because the approach relies on a DC electric field, it has the significant drawback of measuring only the β of polar and non ionic molecules.

1.7.2 Hyper-Rayleigh Scattering (HRS):

The HRS technique was developed in the 1990s to address some of the issues with the EFISH approach. Through the use of this novel approach, the properties of some non-traditional NLO active materials in the solutions may be easily evaluated^[20]. Compared to the EFISH methodology, this method has the major advantage of allowing one to measure the value of Hyperpolarizability without actually measuring the field and dipole vector values. EFISH measurements often need a strong, concentrated electric field, which is not necessary for HRS techniques. When a powerful laser pulse, or beam of laser light, is focused on an isotropic solution containing the NLO active molecules, the intensity of the scattered photons with doubled frequencies is measured using HRS. Rapid and dynamic changes in molecule orientations, can disrupt the virtual center of symmetry in the solution even though it is isotropic (similar to centrosymmetric as in solid).

As a result, using this pseudo-asymmetric solution, the second order optical process may be seen. Compared to EFISH, this method has the benefit of not requiring a directed electric field. This means that these methods may be expanded to measure nonpolar molecules and ions. Additionally a nonlinear optical active molecule's different β tensor components can also be obtained^[21].

1.8 NLO Materials:

Recent advances in optoelectronic and all-optical data processing technologies have opened up a wide variety of possible uses for NLO materials. NLO materials fall into two main categories: inorganic and organic NLO compounds. Conversely, hybrid organic-inorganic materials have recently attracted a lot of attention due to their enhanced properties and complementing effects, such high and changeable NLO features^[22].

1.9 A Comparative Analysis Of Organic and Inorganic compounds:

The two basic categories of NLO active materials are inorganic and organic, depending on the type of molecular components included. The advantages and disadvantages of inorganic and organic materials are comparable^[23].

Table 1.1 provides a qualitative evaluation of the benefits and limitations of each. The majority of commercial applications, such as electro-optic devices in the telecommunications industry, nevertheless frequently employ both pure organic and inorganic semiconductor materials^[19]. Examples of inorganic solids that remain the best choices for several NLO-based device applications include LiNbO_3 and KH_2PO_4 . However, a significant trade-off between the reaction time of the medium and the degree of optical nonlinearity is the main drawback of these inorganic systems. Furthermore, the high and difficulty of manufacturing NLO devices using semiconducting materials preclude their extensive commercial use. Additionally, they are not appropriate for a wide range of potential device applications due to their significant absorption, primarily in the visible portion of the electromagnetic spectrum, and poor optical quality.

Table 1.1 Advantages and Disadvantages of Inorganic and Organic Materials^[4]:

Inorganic Materials	
Advantages	Disadvantages
Largest Bulk Susceptibilities	Absorptions in visible regions
Compatible physical properties	Poor response times
	Degradative photorefractive effects

organic materials	
Advantages	Disadvantages
Efficient Molecular Activity	Bulk susceptibilities strongly depends on Non centrosymmetric crystal packing.
Ultra-fast response times	non-centrosymmetric packing of crystals.
Lower dielectric constants	Thermal deterioration brought on by laser radiation
Improved Capabilities Transparency increased	Visible light absorptions brought on by conjugations
Using structural changes to fine-tune activities	

The molecules that make up the bulk components in NLO materials^{[19][24]} of organic kinds are chemically linked and interact with one another through weak van der Waals forces.

Organic

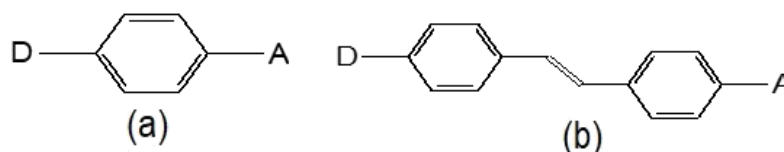


Figure 1.3 Represent Structures of Conventional Push-pull NLO Active Chromophores^[25].

Materials have great inherent tolerability qualities, are easy to fabricate, and are easy to incorporate into devices because of the chemical nature of the adhesions between the molecular units^[26]. Consequently, it is simple to adjust their chemical structures and characteristics for certain NLO applications. Additionally, they exhibit innate synthetic exilities, high optical damage thresholds, low dielectric constants, and more (efficient

or amplified) NLO responses throughout a broad frequency range when compared to their corresponding inorganic materials.

In organic-based NLO materials, the main characteristic is that the visible bulk NLO effects are directly controlled by the NLO behaviors of individual molecule chromophores. The potentialities of organic molecular materials for bulk state characteristics (NLO device applications) can be easily inferred from estimates of their molecular first hyperpolarizability^[27].

Because they provide more immediate advantages than their inorganic equivalents, organic materials are thought to be more suitable for technological applications.

The evolution and future of organic materials are thoroughly examined here in light of the present topic of this dissertation. As preferred chromophores, push-pull systems have been the main subject of research in the field of organic-NLO from its inception. The donor (D) and acceptor (A) in these push-pull forms of NLO-active chromophores are frequently connected (or separated) by an intervening or bridge p-backbone. Figure (1.3) shows two common chemicals in this class. Since these compounds may show significant charge transfers, they are also believed to be effective NLO materials at the molecular level, according to studies. Adding additional electronic asymmetry to the molecular systems may drastically change (or enhance) β in push-pull systems, as is clear from almost all of the prior works. Modifying the Donor-Acceptor(D-A) pairs, extending the conjugation between the D and A, or using strong donating/accepting groups are common strategies^[14].

Two easy methods to carry out these asymmetric manipulations, sometimes referred to as asymmetric magnifications, are (bond-length change). At a laser light wavelength of 1.19 nm, the expected β -values for a few common molecular chromophores are shown in Table 1.2.

Table 1.2 First Hyperpolarizabilities β of Selected Molecular Chromophores' in $(10^{-30})esu$ [4].

β	Category	Typical molecules
0.001 - 0.1	Not very important	triatomics and diatomics (like HCl)
0.1 - 1.0	Little	tiny chemical compounds, such as urea
1.0 - 10	Simple	Benzenes with push-pull
10 - 100	Big	Stillbene push-pull (DANS)
100 - 1000	Very big	colored molecules, extended π -organics,

* Note that the β depends on the choice of input frequency of the laser source. Moreover, changes in molecular structures themselves can significantly affect NLO responses^[28]

1.9.1 Organic/Metallo-Organic Based NLO Materials:

The rapid development is unavoidable, and information-related technology innovation is receiving greater attention as broadband networks expand globally. In this new era of information technology innovation, the emergence of new application sectors, is an increasing demand to enhance the network infrastructure and boost the capacity to process large amounts of data.

Additionally, the bandwidth of optical communication networks is becoming more and more constrained. When

designing optical communication networks, the electro-optic modulator is a crucial component. Nowadays, organic NLO materials are the main components of modern electro-optical systems, taking the place of inorganic ones due to their high electro-optical coefficient, quick reaction time, simplicity of processing, and integration capabilities. These materials are also widely used in the THz radiation, medicinal, and high-speed communication industries^[29]. Among the most advanced materials on the market now are NLO materials, which can alter the frequency of laser light interactions^[30]. Considering the wide range of uses for NLO materials in optoelectronics, photonics, and medicine, this field of study is still in its infancy^[31]. A lot of research has recently been done to examine alternative NLO materials, such as molecular dyes, polymers, and nanostructures, because using inorganic NLO crystals is quite expensive. Imaging, photodynamic treatment, and sensing are examples of growing technologies that are always looking for new, highly effective, and reasonably priced materials^[32]. Organic molecules are special because of their versatile design, high NLO sensitivity, and inexpensive production costs. Organic dyes have become popular because they are simple to produce, purify, and are generally environmentally benign. Recently, scientists have been interested in the appealing NLO response of organic compounds having electron donor (D) and acceptor (A) groups connected by π -conjugated bridges. By positioning the appropriate D, A units, and π -bridges, one may precisely control the intramolecular charge transfer (ICT) between the withdrawing group(A) and

electron donor (D), hence altering the NLO characteristics of D- π -A compounds.

Recently, it has been demonstrated that these dipolar D- π -A structures have significant hyperpolarizabilities. In general Stronger electron-donating and electron-withdrawing capacities are correlated with higher values.

Consequently, NLO chromophores have been designed and synthesized using a range of potent electron donors and acceptors. As a result, the connected length and the characteristics of the donor and acceptor subunits must be taken into account. High photoelectric coefficients, low dielectric constants, low production costs, and flexible design are all advantages of organic NLO materials. The macroscopic characteristics of NLO materials are often caused by the hyperpolarizability of the NLO chromophore Optimizing organic NLO frequently starts with the design and modification of the structure supplya high level of microscopic hyperpolarizability (β values) is required for the efficient use of NLO chromophores in device manufacturing. Additionally, they can guarantee the effective translation of microscopic data to macroscopic electro-optical (EO) coefficients. Two aspects of chromophore design and synthesis have received a lot of attention lately in an attempt to obtain high hyperpolarizability: Chromophores with extreme polarity are created by improving the chemical structure in order to increase the efficacy of the switching response and reduce dipole-dipole interactions.

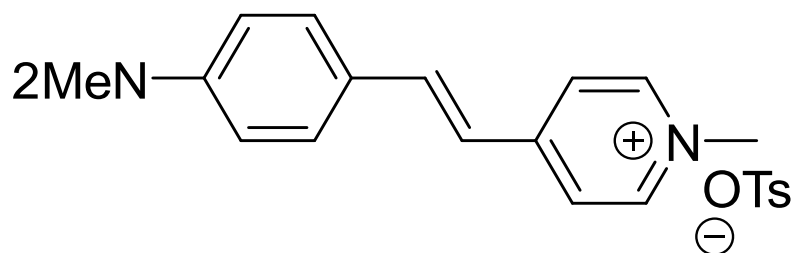
Dalton et al. were the first to propose the site-isolation principle and the idea of a "appropriate isolation group"^[33].

were successful methods, as were Zhen Li and others, for improving translation efficiency for high EO coefficients^[34].

Several notable accomplishments were demonstrated by Jindong Luo and Alex Jen et al. by improving the bridge structure and modifying the electron donating and withdrawing strengths. NLO chromophores^{[35][36]} Dimethylamino-N-methyl-4-stilbazoliumtosylate (DAST) crystals are the only commercially accessible organic NLO chromophores used as THz emitters for spectroscopy (figure 3). Its greater NLO capabilities and other inherent benefits are the cause of this. However, stronger THz radiation than DAST's is needed for several applications in astronomy, communication, testing, defense, and security. The DAST molecule is made up of a non-polar tosylate anion and a positively charged stilbazolium chromophore^[37]. Strong methyl pyridinium electron-acceptor and dimethyl amino electron-donor groups (D- π -A) characterize the stilbazolium chromophore, which is a dipolar molecule.

This D- π -A shape has a low dielectric factor and a high initial hyperpolarizability (β).

THz radiation is generated in the DAST crystal using second order NLO techniques including optical rectification or differential frequency methods. The substantial initial hyperpolarizability (β) of the DAST crystal is the physical fact that underlies this method^[27].



Scheme 1.1 Sylate-forming Structure of Dimethylamino-N-Methyl-4-Stilbazolium (DAST)^[38]

Researchers are trying to identify which possibilities might be the best NLO materials by examining more thoroughly how metals affect the properties of organometallic complexes. This is because a phosphorescence with singlet-triplet intersystem crossover has a significantly better quantum efficiency when the metal is attached to the organic chromophore. Because organic complexes combine the characteristics of inorganic and organic complexes, their NLO properties have been carefully studied, increasing the possibility for the development of high performance NLO materials^{[39][27]}. These include metal phthalocyanine, metal porphyrin, metal iridium, metal carbonyl, metal olefin, metal polyacetylene polymers, and other compounds present in NLO materials. Due to their outstanding performance, six-coordination, diverse valence states, and coordination forms, iridium (III) complexes will undoubtedly be the primary focus in future research on second-order NLO materials^[40]. C.C. Frazier and colleagues firstly described the second harmonic effect of metal organic compounds in 1986. since then additional non-linear optical (NLO) have been identified in metal organic compounds. Its chemical composition directly affects the hue and NLO properties of the metal-organic combination. They are better to NLO materials

composed of simple organic compounds because metal-organic complexes may take on a range of forms due to the diversity of their ligand metals.

Metal atoms have unique optoelectronic properties that depend on their d or f electron numbers, coordination numbers, and oxidation states, allowing them to form a wide range of three-dimensional structures.

For example, the addition of metal atoms can result in magneto-optical and electro-optical phenomena because they combine optical, electrical, and magnetic characteristics.

The formation of a non-centrosymmetric crystal can occur from a chiral center created by the redox modification of the central metal. Compared to other types of compounds, such as metal-organic complexes, show increasing polarizability, absorption bands, and energy between the ground state and excited state. In addition, photons have the ability to go from metal to ligand and back again. The material has a faster photoelectric reaction time due to the little level differential. Developing and synthesizing ligands with unique structures will facilitate the development of more intricate studies.

There have been several non-linear review studies conducted on metal complexes, including rhodium, zinc, and others. Few organic compounds containing iridium metal have been evaluated, although^[33]. Organic NLO materials have a significant role in the creation of photonic platforms, according to the evidence currently available^[25]. Using organic second-order NLO (also called organic electro-optic), or (EO) polymers effectively has been very helpful for photonic applications^[34].

Plasmonic-organic hybrid (POH) modulators using organic EO materials offer efficient EO manipulation of micrometer footprints by circumventing the speed limitations of both photonics and electronics through the use of silicon photonics, organic electro optics, and plasmonic sub-wavelength light confinement^[41]

1.10 Chromophores D- π -A:

NLO organo-based chromophores often exhibit delocalized electronic charge due to their bond architecture. The intramolecular electrostatic interaction between the electron-accepting moiety (A) and the electron-donating moiety (D) through the spacer-linker is linked to initial hyperpolarizability (β_0). Frameworks of various types, such as D-A, D- π -A, D- π - π -A, D-A- π -A, D-D- π -A, D- π -A- π -D, and A- π -D- π -A, have been mentioned in the literature^[42]. Understanding the characteristics of the D and A moieties is necessary to create a good NLO response since the literature has a wide variety of -linkers. To create A-D- π - π - π -A and D-A-D- π - π -A organic molecules, a push-pull configuration has been developed using the appropriate D, π -conjugation spacers, and A^[29].

By affecting the charge transition, expanding the transition range at longer wavelengths, restricting charge recombination, boosting the asymmetric electronic distribution, and considerably lowering the HOMO-LUMO energy gap, these push-pull designs enhance the NLO responsiveness.

The ideal materials for NLO, according to the literature, have lengthy conjugated structures. Utilizing a range of

methods, such as the electron push-pull mechanism, extended electron conjugated systems, octupolar molecule synthesis, and changing the amount and configuration of metals in various complexes, high performance NLO materials have now been created. Materials may be made more NLO sensitive by increasing the number of electrons in a system, which influences the NLO characteristics and increases hyperpolarizability.

This method is a relatively new one. Previous researches have shown that the system with additional electrons might be a source of inspiration for novel design techniques for special NLO materials^[10]. According to this viewpoint, advanced NLO materials are emphasized as electronic and electron-rich alkaline. The adsorption of alkali metal atoms onto different nanostructures is a practical way to add more electrons to a system.

A variety of NLO materials are produced in this industry using both theoretical and experimental design^[42].

1.11 Changeable NLO:

Numerous experimental and theoretical studies have focused on a range of second-order organic NLO materials during the past 20 years due to their many applications in optical computing, optical data transfer, and electro-optical systems^[43]. Compared to inorganic NLO materials, organic materials have stronger intramolecular charge transfer, improved optical frequency transform, increased thermal stability, and faster reaction times. Moreover, switchable "ON" and "OFF" NLO behavior is shown by organic NLO materials, which is often associated with their capacity to reversibly transition between two stable states. These materials' switchable behavior is frequently caused by the oxidation and reduction processes^[44], changes in

pH^[45], or variation in light and temperature which are essential for their operation^[46]. Over the past 20 years, several studies have been carried out to identify novel switchable NLO materials because of their potential for usage in optical device applications^{[47][48]}. It is essential to find novel materials with remarkable switching capabilities and nonlinearities.

1.12 Polyoxometalates (POMs):

Polyoxometalates have emerged as a priority in NLO material science design. Numerous functional groups found in organic molecules can be utilized to produce a broad spectrum of distinctive NLO materials^[48]. In molecular electronics, one of the main objectives has been to use individual molecules as possible units in nanotechnology (moletronic). One of the most crucial worldwide concerns to solve as future electronic systems shrink to nano and subnanometer (molecular) sizes is the development of high-performance and thermally robust molecular components (such resistors, rectifiers, or memory). Particularly interesting for the development of molecular NLO materials are organic and organometallic compounds having electron donor and acceptor groups joined by a p-delocalized backbone (D- π -A). However, the main barriers to the NLO enhancement of both organic and metalloorganic materials are the trade-offs between non-linearity and transparency.^[49] Nevertheless, POMs are inorganic compounds that have garnered a lot of interest because of their special qualities and wide range of uses, which include memory, capacitors, catalytic magnets, energy conversion (electrochemical cell), and more. Research on their potential as electronic materials began in 1998. Numerous studies have been conducted recently to examine the electron-transport characteristics of POM-made films and their possible

use in memory and other electronic devices^[44].

Many POMs exhibit redox behaviour, which is the ability to take on one or more electrons without altering their structural composition.

The unique design and potential applications of POMs derived from organic materials have piqued the curiosity of many. These hybrid systems are expected to combine and strengthen the organic component and POM cluster properties, perhaps leading to synergistic effects. The three main types of POMs are seen in Figure 4: hetero polyanions, isopolyan ions, and large nanoscale poly molybdate clusters. Isopolyan ions can include just one kind of high-valent group 5 or group 6 transition metal ion. It is now known that there are about 30 isopolyan ions, the best studied of which are octa molybdate and Lindqvist. Using the synthetic approach created by Klemperer and colleagues, the Lindqvist structure, hexamolybdate ion $[\text{Mo}_6\text{O}_{19}]^{-2}$ high thermal and chemical stability, may be synthesized^[50]. Six edge-sharing MoO_6 is composed of densely packed MoO_6 octahedra. The entire structure exhibits octahedral symmetry. They are interesting building blocks because of their redox properties and single-electron uptake. the movement of electrons^{[51][52]}.

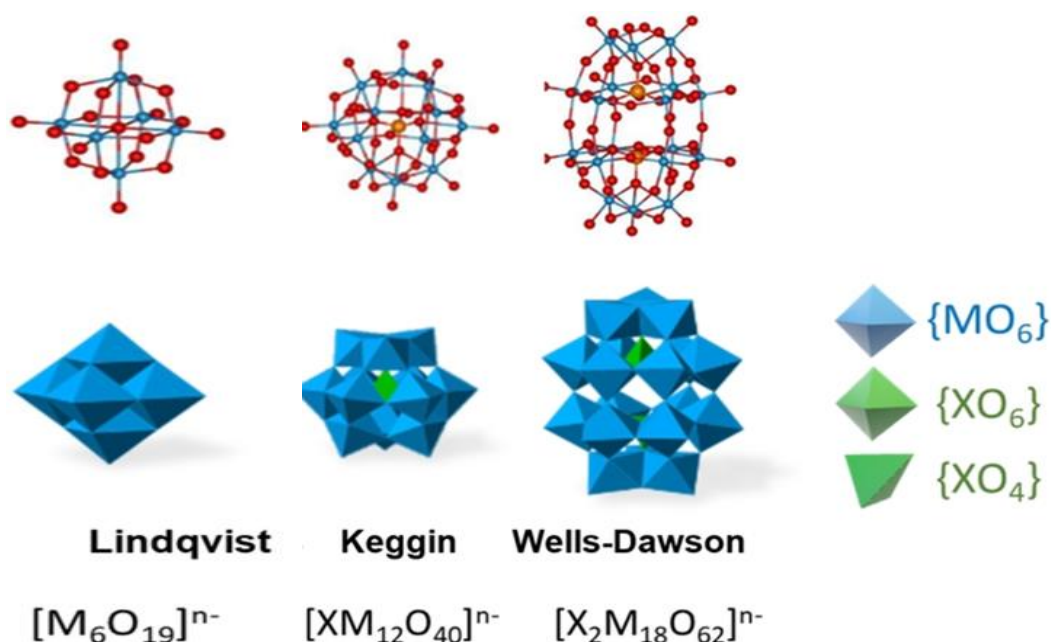


Figure 1.4 Common structures of polyoxometalates: Bull- and – stick and polyhedral Representations of the three most prevalent poly or me folate anions :

(a)anion (Lindqvist)[Mo₆O₁₉]ⁿ⁻ (b)[α-{XO₄}M[12O₃₆]

(c)[α{XO₄}₂M[8O₅₄]_γ-keggin anionz - wells -Dawson configuration ^[38].

1.12-1 Derivatives of Lindqvist-Organoimido:

It is believed that organoimido derivatives—POMs coupled with small organic functional groups—are the fundamental building block for more intricate and durable POM-organic hybrid materials. POMs can be functionalized in various ways to produce organoimido compounds ^{[35][51]}.

Recently, the hexamolybdate ion $[Mo_6O_{19}]^{2-}$ has been the focus of most of the study on the organoimido-POM compounds. Ingvar Lindqvist, a Swedish scientist, first released the Lindqvist in 1950. Among conventional POMs, it is the simplest and easiest to understand. Its general formula is. $[Mo_6O_{19}]^{2-}$ Due to its well-defined Lindqvist structure, chemical stability, and ease of production, the hexamolybdate ion is one of the most well-known

POM clusters. In the Lindqvist structure, an octahedral cage composed of six metal and eighteen oxygen atoms encircles a core oxide ion. All six metal atoms are found in the octahedral environment.

They coordinate three times to one terminal oxygen atom in addition to the central oxygen atom to create a terminal metal-oxo group (Mo). They also share four additional doubly bridging oxygen atoms (μ 2-O atoms). A variety of nitrogenous species, such as imido, diazoalkyl, and azenido groups, can directly replace the terminal oxygen atoms in hexamolybdate due to the molybdic groups (Mo O) being sufficiently reactive. Among these organic-inorganic hybrid systems, Lindqvist hexamolybdate organoimido derivatives have attracted a lot of attention. The remarkable optical, catalytic, electrical, and magnetic properties of these compounds are a result of the strong interactions between d-p orbitals and p-p electrons. Due to its simple to process, this inventive device can produce a wide range of complex hybrids. Furthermore, they share a molecular structure with metal oxides at the nanoscale, which are better suited for device applications. This suggests that the POM is more promoted than the organic species because massive current densities are predicted to flow through these molecule clusters even at low bias voltages. One of the more interesting types of POMs that have been chemically functionalized is an organoimido derivative. A new class of electronic hybrid materials might be created by delocalization of the organic p electrons on the POM cluster, in addition to the exceptional stability of the imido metal-nitrogen bond, which permits further structural modification of the organic component attached to the cluster^[6]. They have attracted particular attention because the organic electrons in the organoimido derivatives of Lindqvist type Hexamolybdate $[\text{Mo}_6\text{O}_{19}]^{-2}$ may extend their conjugation to cluster d electrons, resulting in strong d-interactions. Many organoimido compounds are present in POMs of the Lindqvist

hexamolybdate type. In essence, one or maybe all six of a hexamolybdate ion's terminal oxo groups can be substituted by various organoimido ligands. Terminally substituted mono- and even multi-functionalized organoimido derivatives of POMs have been produced using a range of imido-releasing substances ^[53]. A few years ago, Matta et al. guided the POM cluster of hexamolybdates to facilitate the functionalization of POM cages. The selective synthesis of difunctionalized organoimido hexamolybdate derivatives was investigated by Xu et al. via a novel and very effective method. Organoimido derivatives of POMs may be helpful for producing covalently tailored hybrid composites based on POM, according to research by Lu et al. Due to the strong electronic interactions between the unsaturated organic chains and POM clusters (hexamolybdates), these hybrids are fascinating electrically effective materials. The electro-activity of POMs allows them to be coupled with electrically active organic groups to create materials with a wide range of potential uses in biological materials, sensors, solar energy conversion, and molecular device processes^[43]. Matta did a fantastic work. Three distinct reaction types have been devised by Proust and Errington and collaborators to synthesis hexamolybdate imido derivatives. Aromatic amines, isocyanates, and phosphamides are examples of memorializing reagent reactions. The six terminal oxygen atoms of the hexamolybdate cluster (as well as occasionally some bridging oxygen atoms) can be completely replaced by organoimido ligands using these techniques. The structures of monodi , and multi-substituted organoimido derivatives of hexamolybdate have been determined and synthesized in recent investigations ^[54].

1.12.2 Literature survey On Organoimido-Lindqvist as NLO Materials:

POMs have emerged as new and promising NLO materials that may be utilized to produce D- π -A chromophores with organic donors due to their high electron acceptor capacity. There are several charge-transfer salts that have been created.

When POM anions are mixed with organic and organometallic cations, these salts are invariably produced. However, these charge transfer salts' relatively weak organic and inorganic interactions in the solid state have prevented an efficient electron transfer between the two components [44]. On the other the hand, heterometallic POMs are especially intriguing because they provide a basis for comprehending the role of mixed oxide catalysts and a unique opportunity to investigate the reactivity of isolated heterometal sites embedded inside a matrix of another metal oxide at the molecular level^[55]. Only a small number of NLO-active materials contain POM anions, and they are all focused on the second-order NLO response, despite the fact that chiral POM-based materials have demonstrated remarkable NLO responsiveness in recent theoretical and experimental investigations^[46].

The organoimido derivatives of POMs, particularly those of the Lindqvist type, make excellent NLO crystals .this is primarily due to their strong D-synergistic effect between the delocalized electrons of the organic moiety and the vacant p-d orbitals of the POM group. These compounds exhibit strong electronic transitions, versatility due to a wide range

of metals, and ease of modification to set the stage for desired applications. Following the pioneering work of Yan Likai and her colleagues, many studies have been carried out to better understand the NLO response of POM-based hybrid materials. The NLO response of replacing hexamolybdate with organoimido was initially assessed in this study employing a variety of organic-inorganic hybrid systems^{[46][48]}. Recently, a lot of emphasis has been focused on the NLO properties of this kind of material. When comparing these hybrid organic-inorganic materials to crystals that are entirely inorganic or pure organic chromophores, the second-order NLO response may be enhanced due to the change in charge transfer direction caused by the lengthening of π -conjugation or the transition from a single ring to a double ring^[56].

Due to their potent d-d interactions between the organic delocalized electrons and the cluster empty d orbitals, strong electronic transitions, versatility with respect to a range of metals, and ease of modification to provide building blocks for particular purposes (noncentral symmetric molecules), POM-based organic and inorganic hybrid materials especially organoimido-Lindqvist derivatives are excellent candidates for use as NLO materials ^[15]. But their optical qualities have so far only been addressed by calculations based on enormous second-order NLO factors. These materials are great candidates for use as redox switchable NLO chromophores because of the clear, quick electrochemistry of the Lindqvist anion and this prediction. The two-photon absorption activity and the first experimental second-order NLO activity using the HRS technique for donor-functionalized arylimido-POMs were recently reported by Al-Yasari et al.

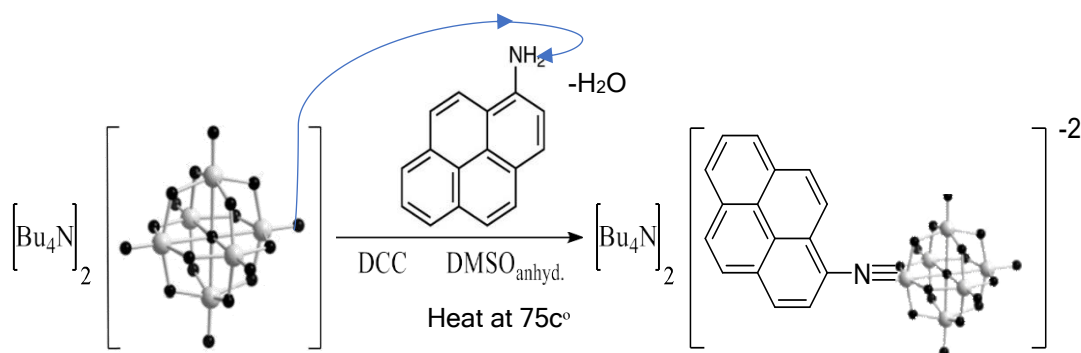
The systems under investigation exhibited strong NLO responses with significantly superior transparency/non-linearity trade-offs than comparable organic systems because of the high charge transfer transitions and strong electronic linkages between the POM clusters and organic moieties^[57]. NLO responses are frequently greater than those obtained from comparable structures, such organic acceptors, according to the research .DFT was recently used to obtain the initial hyperpolarizability β -values for these derivatives, which Champagne and colleagues compared with experimentally measured ones^[58]. The results demonstrated that the model used to calculate β -values was valid, with a good agreement between the estimated and experimental values these findings have heightened more interested in developing POM-based NLO chromophores with notable NLO responses. As crucial building blocks, pyrene-appended formyl pyridine and bis (amino phenyl) BODIPY were employed to create a brand-new, bright metallo-supramolecular capsule.

1.13 Pyrene-based Donors :

Pyrene and its derivatives may create excimers through π - π interactions, and are known for their long fluorescence lifetimes, high quantum yield, and sensitive vibronic fine structure.^{[59][60]} Because of their long-lived excited states and massive quantum yield of fluorescence, pyrene and its derivatives are undoubtedly interesting choices for studying and comprehending the electron transfer mechanism in organic-functionalized POMs.

While some pyrene-grafted POMs have demonstrated potential shown promise for use in sensors, catalysts, as well as certain special optical properties,^[61] The linkers between POMs and pyrene in these hybrid materials often fail to facilitate electronic "communication" between the two constituents. Organic donors must be directly bonded to POMs by a brief, rigid bond in order to increase "communication" efficiency"

This research indicates that the imido group might create new photophysical properties and provide an opportunity to study the mechanism of electron transfer in organic functionalized POM hybrid materials by fortifying the bonds between the highly delocalized π - π electrons of the pyrene ring and the d orbital of the POM skeleton^[62], is a novel pyrene imido derivative of hexamolybdate that we introduced using the DCC coupling protocol 24. Both theoretical and experimental approaches were employed to examine the photophysical characteristics of the hybrid cluster, as shown in the following scheme:



When: DCC is N, N-Dicyclohexyl Carbodiimide, DMSO is Dimethyl sulfoxide

Scheme 1.2 Structural Representation of Linkers Enabling Electron communication Between POMs and Pyrene Units in Hybrid Materials^[63]

1.14 Aims of Study:

The primary objective of this study is to investigate the NLO properties of POM complexes based on pyrene derivatives and to synthesize new compounds by structurally modifying pyrene groups in the manner described below.

1. To design and evaluate novel hybrid materials based on POMs functionalized with potent donors, specifically pyrene donor groups and their derivatives, as switchable NLO compounds using quantum chemistry (DFT).
2. To enhance the electro-optical characteristics of the system under study.
3. To examine the stability of the derivatives and how they could change NLO properties by examining the adjacent methylation ortho the imido-groups.
4. To explore how the pyrene structure is affected by phenyl, alkyl, and other substitution groups, which affects their donor capacity and, in turn, adjusts the transfer of charge from ligand to POM.

CHAPTER TWO
COMPUTATIONAL
THEORY AND
METHOD

2.1 Computational Chemistry:

Using a well-defined set of tools, computational chemistry uses the power of a computer to examine a wide range of scientific topics, including those pertaining to chemistry, chemical biology, chemical physics, materials chemistry & physics, etc. The employment of suitable mathematical tools to solve the quantum mechanical equation is the basic concept behind all computational chemistry techniques.

More and more, computational chemistry is being utilized to study the properties and structure of both tiny molecules and bulk materials. Because of the arrival of very efficient computers, computational chemistry has expanded to include all scientific disciplines. In addition to helping many experimentalists comprehend their job, they can also learn a lot of challenging and fascinating ideas from computational chemistry^[64]. With the development of computational chemistry, practically every scientific field may now benefit from its use in quantum mechanics to describe atomic orbitals, with a focus on Schrödinger's equation. Its use in computational chemistry, including Density Functional Theory and Hartree-Fock approaches, is then explained. The principles of inverse design will be covered in our last section, along with how they may enhance the use of computational chemistry to speed up the development life cycles of novel chemicals and materials ^[65].

2.2 History and Software of Computational Chemistry:

The advent of a number of easily accessible computer programs is partly responsible for the growing tendency in recent years toward the use of computational simulations of chemical processes. As a result, researchers no longer need a degree in theoretical chemistry to understand how the interactions inside the beaker are described by theory. While ^{[66][67]} computational quantum chemistry is a complex fusion of chemistry, physics, mathematics, and computer science. To avoid doing work on precarious groundwork, it is crucial to have at

least a rudimentary grasp of the mathematics behind these calculations. Chemistry defines the nature of the problem while the question. Physics defines the laws that govern the chemical system. Mathematics provides a numerical representation of the issue. As shown in the following figure:

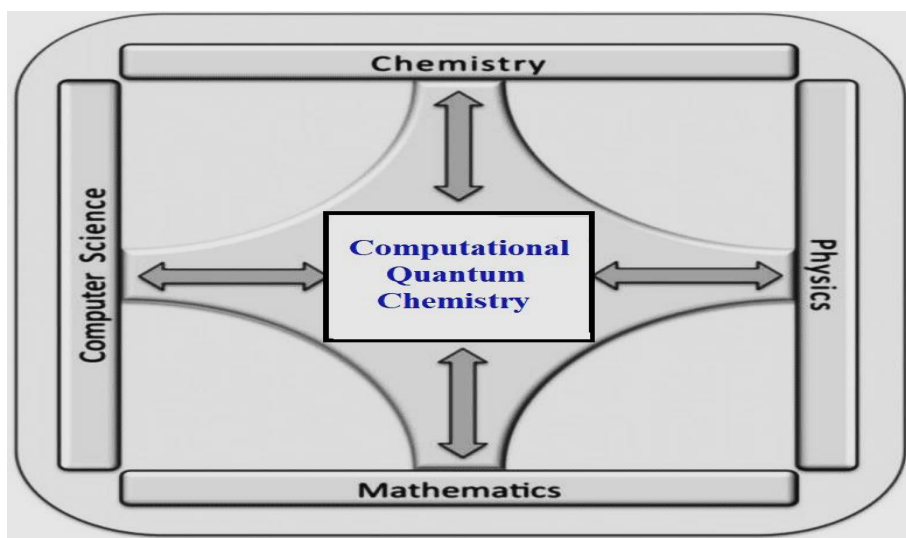


Fig. 2.1 Interdisciplinary Foundations of computational chemistry^[68]

In the past, only experts with access to high-performance computer resources, advanced software development and numerical techniques, and a solid grasp in the underlying quantum mechanical models were allowed to work in computational quantum chemistry. These days, non-specialists may do complex quantum chemistry calculations with the aid of powerful desktop computers and easily accessible software.

Hoffmann's theories have been expanded upon in recent decades by computational chemistry as it relates to organometallic chemistry, which has increasingly sought to take advantage of the advanced instruments created and made accessible by theoretical chemists^[69]. The development of mathematical model With the introduction of electronic computers following World War II. Although there had been attempts in the 1920s to solve Schrödinger's equation mechanically, there was not enough computing power to provide reasonable approximations of the equation for multi-electron elements. Scientists would learn how to maximize this new technology in the next decades^[70].

2.3 Methods of Computation:

Every calculation pertaining to linear light absorption properties, geometry optimizations, and first hyperpolarizability NLO (tensor components) was carried out using the Gaussian16^[71] suite24 on the High-Performance Computing Cluster, which is made possible by the Research and Specialist Computing Support service at the University of East Anglia.

Geometric optimizations were performed using the 6-311+G(d) basis set for (C,H,N and O) the range-separated hybrid functional ω B97XD, and the LANL2TZ basis set for Mo atoms, in accordance with the methods outlined in the literature by Rtibi et al^[7], where they have performed benchmarking and found that (6-311+G(d)/LANL2TZ or LANL2DZ) with ω B97XD is the best level of theory for organoimido Lindqvist derivatives. The SMD solvation model created by Truhlar and colleagues was applied to take solvent effects into consideration. This mixed basis set was created using the Gaussian programming language's GEN phrase.

In recent years, computational chemistry study has increasingly adopted these mixed basis sets. For the study of transition metal-containing systems, it has become usual practice to combine these two basis sets using density functional techniques^[72]. Using the solvent acetonitrile, calculations were first applied to the gas phase and subsequently to single point energy. Using the TIGHT convergence criterion, 1.5×10^{-3} Hartree/Bohr or Hartree/radian were applied to the remaining atomic forces at the same theoretical level. Linear optical computations were performed using the SMD model for the acetonitrile solvent with ω B97XD/ 6-311+G (d, p)/LANL2TZ. Using a 50:50 split between singlet and triplet, 100 lowest energy transitions were calculated, and only space absorptions were determined to be meaningful.

The NLO properties were applied using the same level of functional and basis set as optimization and linear optical computations with acetonitrile solvent. Corresponding solutions were obtained under these conditions.

Additionally, HOMO-LUMO analysis was carried out to gain a better understanding of the charge transfer process and the source of the compounds' NLO activity.

2.3.1 Hyperpolarizability and the Analysis of Two-State Models:

Dipole polarizability (α) and first-order hyperpolarization (β) were calculated using the following formula:

However, the following formulae were employed to determine static hyperpolarizability (β):

$$\alpha = \frac{1}{3}(\alpha_{XXX} + \alpha_{YYY} + \alpha_{ZZZ}) \dots\dots\dots(\text{Eq.2.1})$$

However, the following formulas were applied to determine static hyperpolarizability (β_0).

$$\beta_X = \beta_{XXX} + \beta_{XYY} + \beta_{XZZ} \dots\dots\dots(\text{Eq.2.2})$$

$$\beta_Y = \beta_{YYY} + \beta_{YYZ} + \beta_{YXX} \dots\dots\dots(\text{Eq.2.3})$$

$$\beta_Z = \beta_{ZZZ} + \beta_{ZXX} + \beta_{ZYY} \dots\dots\dots(\text{Eq.2.4})$$

$$\beta_0 = \sqrt{\beta_X^2 + \beta_Y^2 + \beta_Z^2} \dots\dots\dots(\text{Eq.2.5})$$

Furthermore, when the incoming light is horizontally ((β^2_{ZXX})) or vertically ((β^2_{ZZZ})) polarized, the SHG responses—more specifically, the HRS initial hyperpolarizability (scattered intensities) $\beta_{HRS}(-2\omega, \omega, \omega)$ and the static β_0 —were calculated using the following equation:

$$\beta_{HRS}(-2\omega, \omega, \omega) = \sqrt{\beta_{ZZZ}^2 + \beta_{ZXX}^2} \dots\dots (\text{Eq.2.6})$$

For optimum geometries with ω B97XD, TD-DFT was utilized to compute the β -responses and β -tensor components of both static β_0 and frequency-dependent β_{HRS} (at 1064 nm incidence wavelength) utilizing the 6-311+G(d)/LANL2TZ basis sets and SMD method to include solvent effects. The push-conjugated system's β tensor usually has just one diagonal tensor component (β_{ZZZ}), therefore β_{HRS} may be computed as follows:^[73]

$$\beta_{ZZZ} = \sqrt{\frac{35}{6}} \beta_{HRS} \dots\dots\dots(\text{Eq.2.7})$$

Therefore, both β_{ZZZ} and β_0 responses have been recorded in this study.

The poly oxo metalate-based derivatives may be approximated using a two-state method, where $\beta_{ZZZ} = \beta$, which is provided by:

$$\beta = \frac{6\Delta\mu_{ge}(\mu_{ge})^2}{(E_{MAX})^2} \dots\dots\dots(\text{Eq.2.8})$$

where μ_{ge} is the transition dipole moment and the difference in excitation energy between the ground (g) and excited (e) states is $E_{max}=E_e-E_g$. The dipole moment difference between the ground (g) and excited (e) states is $\mu_{ge}=\mu_e - \mu_g$. Following the procedure described by Guido et al. [74]

2.4 Quantum Mechanics:

The ren owned Double-Slit experiment in 1801, which demonstrated that electrons may behave as either solid particles or waves depending on whether they were being seen, is credited with giving rise to quantum mechanics^[76]. Since then, science has expanded significantly, especially in the 20th century, when significant discoveries like the Higgs Boson and general relativity transformed knowledge of the cosmos and made scientists like Erwin Schrödinger and Albert Einstein well-known.

The research on how electrons operate inside atoms is the most pertinent. In turn, Niel Bohr's model of the atom^[66].disproved the initial theory that electrons moved in distinct orbitals around the atomic nucleus, similar to how planets circle stars. In this case, electrons could only orbit at certain, quantized distances; the orbital is the next potential path each electron may take in its orbit.

This expands on the research of other important scientists, such as Boltzmann, Planck, Einstein, and others^[64]. Bohr's model has several problems, one of which is that it ignores the uncertainty principle that the Double-Slit experiment illustrates. Since electron positions is specified using probability through Schrödinger's equation (Eq.2.9), which uses wavefunctions to describe electrons. As a result atomic orbitals must be appro abed. Although quantum mechanical principles rather than classical or bits of the probability of

discovering an electron within its atomic orbital is 100%, the exact location of the electron through the electron within the orbital at any particular moment cannot be predicted with certainty^[77].

$$\Psi(r, \theta, \varphi) = R(r), Y(\theta, \varphi) = NR_{n,1}(r)P_1^m(\cos\theta)e^{im\varphi} \dots\dots\dots(\text{Eq.2.9})$$

where:

$\Psi(r, \theta, \varphi)$ = full description of the electron wavefunction in three dimensions

$R(r) = R_{n,1}(r)$ = radial component (z-axis contribution)

$Y(\theta, \varphi) = P_1^m(\cos\theta)e^{im\varphi}$ angular component (x- and y-axis contribution)

N = total number of constants.

n = main quantum number (1, 2, ...)

l = azimuthal quantum number (0, 1, 2, ..., n-1).

m = magnetic quantum number (-n-1, ... -2, -1, 0, 1, 2, ..., n-1)

To solve for specific values of n and l , the radial components can be expressed using its full equations: For the angular component, we must further split

$$R_{n,1}(r) = \frac{1}{2}e^{-\zeta} \zeta^{1+1} V(\zeta) \dots\dots\dots(\text{Eq.2.10})$$

$$\zeta = \frac{1}{0.529n} \dots\dots\dots(\text{Eq.2.11})$$

For the angular component, we need to further separate $Y(\theta, \varphi)$ into the polar and azimuth equations before solving for l and m :

$$Y(\theta, \varphi) = \Theta(\theta) \cdot \Phi(\varphi) \dots\dots\dots(\text{Eq.2.12})$$

$$\Theta(\theta) = P_1^m(\cos\theta) \dots\dots\dots(\text{Eq.2.13})$$

$$P_1^m(x) = (1-x)^{\frac{|m|}{2}} \left(\frac{d}{dx}\right)^{|m|} p_1(x) \dots\dots\dots(\text{Eq.2.14})$$

$$\Phi(\varphi) = C_1 e^{im\varphi} \dots\dots\dots(\text{Eq.2.15})$$

Since Schrödinger's equation treats each wavefunction as a standing or stationary wave its time-independent form ($\hat{H}\psi = E\psi$) is generally more traceable than its time-dependent form, ($i\hbar(\partial/\partial t)\Psi = \hat{H}\Psi$) which oscillating wavefunctions due to the constantly changing probability of finding an electron at a given point.

The equation also describes atomic orbitals where electrons are likely to be

to and orbital form, or the route as they round the atom, is also described by Schrödinger's equation, which correctly depicts an electron as a wave. Schrödinger's equation can be solved manually only for the simplest elements, such as hydrogen and helium, due to the increasing complexity of higher energy orbitals, especially d and f orbitals; As atomic system grow more complex especially in heavier elements heavier atoms require the assistance of a computer.

Bohr's model also explains why specific molecules or elements emit light at specific wavelengths. This is connected to UV-Vis absorption. A quantized packet of light must be absorbed in order to elevate electrons from their distinct orbitals to a higher order orbital. Usually, these excited electrons return to their initial orbital when the absorbed energy is released as electromagnetic radiation. As a result, the wavelength of light emitted is found using equation 2.16.

$$E = h / \lambda \dots\dots\dots (Eq.2.16)$$

in where $h = 6.626 * 10^{-34}JS$, $\lambda = \text{wavelength (nm)}$

The excitation of an electron across the energy dimension known as the HOMO-LUMO gap, from the Highest Occupied Molecular Orbital (HOMO) to the Lowest Unoccupied Molecular Orbital (LUMO), is linked to the first/lowest energy absorption band. Although it usually generates light in the ultraviolet region of the electromagnetic spectrum, this HOMO-LUMO gap can create blue-shifted light when POMs are lowered.

2.5 Quantum Biology:

The study of how quantum events affect biological processes is an emerging area that blends biology and quantum physics. It also has potential use in power generation, health, and materials research^[14]. Our understanding of the physical universe at the atomic and subatomic levels was fundamentally changed by the advent of quantum physics in the early 1900s.

However, its possible effects on biological systems, which function on a completely different scale, were unknown until recently. The recently developed discipline of quantum biology examines the potential impact that quantum

events may have in biological systems in an effort to close this gap. This new branch of research, known as "quantum biology," examines how biological processes could be impacted by quantum physics. Understanding the potential effects of quantum phenomena like superposition, entanglement, and tunneling on the molecular and cellular behavior of biological systems is crucial^[69]. Some events involving atomic and subatomic interactions may need an understanding of quantum physics, even if many biological processes may be described by classical mechanics. Quantum biology seeks to identify and comprehend these quantum events and their impact on biological function.^[78]

2.5.1 Important Turning Points in Quantum Research:

As the following table summarizes, quantum biology has advanced tremendously from the early twentieth century:

Table 2.1: A chronology of quantum research turning points that established the area of quantum biology^[79]

Year	The event *	Importance
Early 20 th century	Development of quantum mechanics	created a theoretical foundation for understanding the properties and relationships of matter and energy at the subatomic and atomic levels.
1920s	Concepts from early quantum biology	Scientists like Niels Bohr and Erwin Schrödinger started investigating the possible applications of quantum mechanics to biological systems.
1960s	Photosynthesis research	The significance of energy transfer mechanisms, which would subsequently be connected to quantum phenomena, became apparent through research on photosynthesis.
1970s-1980s	Enzyme catalysis and quantum tunnelling	Quantum tunneling may be involved in chemical processes in biological systems, according to research on enzyme catalysis.
1990s	Quantum coherence in biological systems	Investigations on the possibility of quantum coherence in biological systems, particularly photosynthesis, were initiated.
2000s	Increasing interest in quantum biology	Researchers' increasing awareness of the potential importance of quantum effects in many biological processes has led to a surge in interest in the field of quantum biology..
2010s	Experimental breakthroughs	Quantum events in biological systems may now be directly observed because to recent developments in experimental techniques. These findings offer strong proof of the importance of quantum mechanics in biological processes...
2020s	Growing interdisciplinary collaboration	Significant advances in the study of quantum biology have resulted from increased cooperation between physicists, biologists, chemists, and other scientists.
Present	Continued advancements	Quantum biology is still being studied, and new findings are being discovered as well as possible uses in industries including energy generation, materials research, and medicine.

2.5.2 Mathematical and Physical Foundations OF Quantum Biology:

Quantum biology is based on quantum mechanics. A basic equation known as the Schrödinger equation defines how the wave function of a quantum system develops over time. Being aware of the wave-particle duality the idea that particles have two different natures is necessary to comprehend quantum activity. they are both waves and particles. The intrinsic constraint of simultaneously detecting a particle's precise location and momentum is highlighted by the uncertainty principle. The ability of quantum systems to maintain quantum coherence. In order to simulate energy transfer processes, the density matrix formalism and Schrödinger equation are employed. The Schrödinger equation, which describes quantum tunneling, is thought to have a role in proton transfer during enzyme catalysis^{[80][81]}.As shown in the following figure.

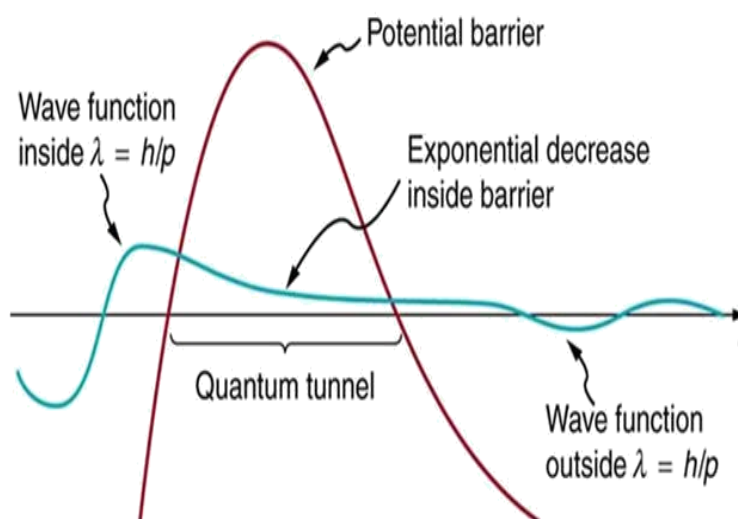


Figure 2.2: Catalysis By Enzymes Via Quantum Tunneling^[82]

2.6 Schrödinger Equation:

Quantum chemistry was first studied in 1926 with the discovery of Schrödinger's wave equation^[7]. The behavior of a physical system's wave function over time is described by the Schrödinger equation. A molecule's electron distribution can be examined using the Schrödinger equation:^[68]

$$\hat{H}\psi = E\psi \dots\dots\dots (\text{Eq.2.12})$$

when \hat{H} is the Hamiltonian operator, E represents the overall energy of the system. ψ is the wave function, describing the spatial position of one electron. The Hamiltonian operates on the wave function to yield the systems

Although Schrödinger's equation has exact solutions, it is very impossible to find them in multi-electron systems because the computations get exponentially more complicated as the number of electrons in the system rises^[83]. The nucleus must be taken into account when the equation becomes a three-body problem with multiple electrons. Since it is impossible to solve these many-body problems exactly theoretically, approximations are required. Using the Born-Oppenheimer approximation, the multi-electron time-independent Schrödinger equation may be solved^[84].

The premise behind this is that although nuclei are inherently stationary, their relative motion may be explained by the fact that they are far heavier than electrons. This makes it possible to calculate the Schrödinger equation's nuclear and electronic components separately.

DFT, ab-initio procedures, and semi-empirical methods are further approximations that may be employed to lessen the Schrödinger equation's complexity. The Latin phrase "ab initio" translates to "from the beginning." Ab-initio techniques are used in quantum chemistry to compute variables, which are parameterized directly from theoretical concepts as opposed to experimental data. Over the past three decades, these techniques have been widely applied in the study of molecules. The goal of computational quantum chemistry is to ascertain the wave functions and electronic energies of every other chemical species, including atoms and molecules. Assuming that the molecule is a collection of positive nuclei and negative electrons sensitive to Coulombic potentials, the Schrödinger equation is solved from first principles, even though a realistic starting structure of the molecule is often required when performing a calculation. When trying to apply ab initio approaches to complex systems, it is

inevitable that approximations will be made to simplify computations ^[85].

Electrical structural techniques may be broadly classified into two categories: Ab-initio and Semi-empirical.

Semi-empirical computations employ experimental data to parameterize their techniques, whereas ab-initio computations are derived from theoretical concepts without the use of actual data. Better results can be obtained with higher quality techniques, even if the cost of computation rises exponentially with the number of atoms. There are scaling factors (N) associated with several popular ab initio techniques, where N is the number of basic functions employed. These variables affect the computation cost of the employed technique and scale exponentially with m . These consist of linked cluster (CC), HF (N), configuration interaction (CI), and many body perturbation theory (MBPT) (N). As a result, the most sophisticated of these techniques are only useful for molecules with 20 atoms or less. The correlation term requires the computing of many determinate wavefunctions rather than a single Slater determinant, which raises the computational cost. Large systems, such those found in organometallic systems, require computations that balance speed and accuracy while applying the appropriate amount of theory to the specific chemical challenge. These variables affect the computation cost of the employed technique and scale exponentially with m . These include many body perturbation theory (MBPT) (N), connected cluster (CC), HF (N), and configuration interaction (CI). Therefore, only molecules with 20 atoms or less can benefit from the most advanced of these methods. Instead of using a single Slater determinant, the correlation term necessitates the computation of several determinate wavefunctions, increasing the computational cost. Large molecular systems computing necessitates finding a balance between accuracy and speed, It which are typical of organometallic systems, while ensuring that the right amount of theory is used for the particular chemical problem. When investigating a variety of isomers and possible catalytic pathways, faster electronic structure simulations are also preferable. DFT is the

most widely used methodology since it displays electron density as a function of the ground state geometry, in contrast to the wavefunction-based approaches that were previously addressed.

2.7 Hartree-Fock Self Consistent Field:

The HF approach is a sophisticated technique that involves using (Eq. 2.13) and adding or ∇ subtracting a constant term to arrive at approximate solutions of the Schrödinger equation (differential equation):

$$\hat{H} = \sum_{i=1}^n \frac{1}{2} \nabla_i^2 - \sum_{A=1}^N \frac{Z_A}{r_{iA}} + \sum_{i=1}^n V_{ri} + \sum_{i=1}^n \left(\sum_{j>i}^n \left[\frac{1}{r_{ij}} - V_{ri} \right] \right) \dots \dots \dots \text{(Eq. 2.13)}$$

When \hat{H} is Hamiltonian Operator, ∇_i^2 is Laplacian Operator, Z_A is Nucleus Charge, r_{iA} is distance between i electron and A nucleus, V_{ri} is coulomb attraction between distance electron, r_{ij} is distance between i electron and j electron,

The following is the physical explanation for this: although neither $\sum_{i=1}^n \frac{1}{2} \nabla_i^2$ nor the word itself are small on their own, the term may become small enough to be ignored with a carefully chosen potential V_{ri} . The total of one-particle terms will be the Hamiltonian once the function V_{ri} has been identified [86].

$$\hat{H} = \sum_{i=1}^n f(i) \dots \dots \dots \text{(Eq. 2.14)}$$

Where

$$f(i) = -\frac{1}{2} \nabla_i^2 - \sum_{A=1}^N \frac{Z_A}{r_{iA}} + V_{ri} \dots \dots \dots \text{(Eq. 2.15)}$$

When $f(i)$ is Fock Operator, the electrons' variables are now separated, the answer becomes clear: $(r_1 \dots r_i)$ will be the result of the one-electron eigenvalue equations' answers.

$$F(i)\phi_K(i) = \epsilon_K \phi_K(i)$$

Electron i experiences the averaged repulsive energy from all other electrons, which is represented by the potential energy operator, v_{ri} . The mean field created by all other electrons moving is, in a sense, effective potential.

A straightforward way to depict the electrons as independent of one another is to

"replace" the complex inter- electronic repulsion with sum of one electron operators $V(r_i)$ as the inter-electronic repulsion term. The independent-electron model is just a rough representation of reality, and it is crucial to remember that quantitative findings are rarely accurate due to the extreme approximations.

2.8 Electron Correlation:

The HF method is based on series of approximations that simplify the treatment of electron interaction. The idea that every electron is an autonomous entity that moves in its "own" averaged potential is false. The presence of any electron 2 near a patch of space inhabited by electron 1 at point r_1 , for instance, is highly unlikely. In contrast to the mean field approximation, electrons move away from one another more. Because of this, the calculated energy is too high, which may be lowered by taking electron correlation into consideration. This raises the question how much of the overall energy of the system is this correlation energy.

It's surprisingly not too high. For example, only about 1% of helium atoms' energy ^[87]. In the case of helium, however, this 1% correlation energy is already equal to 26 kcal/mol, making it crucial for chemical accuracy.

Calculating the Gibbs free energy for the formation and breaking of chemical bonds often require precision of many kcal/mol. Since comparing various energies leads to a far lower error, making such comparisons more reliable.

But when drawing quantitative findings, electron correlation is important and has to be taken into account.

2.9 Density Functional Theory (DFT):

DFT is a widely used quantum mechanical method for examining the electronic structure of many-body systems, including those with solid and gas components. Instead of relying on wave function-based approaches, DFT employs functionals, that is functions of the electron density function, which varies across space.

the DFT Functionals, or functions of another function of the spatially variable electron density, are used instead of wavefunction-based methods to infer the parameters of a many-electron system. The DFT approach is computationally efficient as there are just a few variables and the electron density is seen as a single-body issue. Many-body wavefunction approaches, which give each electron three variables, are far more complicated than DFT. Due to its lower computational cost and equivalent level of precision, DFT is frequently employed for catalyst design instead of ab initio calculations [88]. An electronic structure computation's total energy is expressed as a functional ($E[\rho]$) of the electron density $[\rho]$. The usual form of this functional is as follows:

$$E[\rho] = T_s[\rho] + \int dr v_{ext}(r) + V_H[\rho] + E_{xc}[\rho] \dots \text{(Eq. 2.16)}$$

When ρ is the electron density, $T_s[\rho]$ is Kinetic energy, $v_{ext}(\mathbf{r})$ is (the ions are “external” to the N-electron system), The approximation of Kohn-Sham electronic kinetic energy is represented by the first term, T_s . Using spherical coordinates, the external potential of electron-nuclei coulombic interactions is represented by the value $v_{ext}(r)$.

The third term refers to the Coulomb or Hartree energy for the electron density's repulsion with itself. Interactions between electrons are taken into account by the fourth component, the exchange-correlation functional.

Scientists can now use high-throughput computational materials design to find materials with desired properties in massive data repositories, Due to the substantial improvements in first principles calculations and the quick rise in processing power of contemporary supercomputer systems, it is now possible to either learn directly from data or anticipate crystal structures to build novel compounds with the required attributes.

A compound's structural elements, or functional modules (FMs), that control its properties must be identified in order to effectively screen or predict both organic and inorganic molecules. Design, synthesis, and prediction of new materials can

be aided by a thorough understanding of FMs ^[88]. The electronic (or nuclear) structure of many-body systems, including atoms, molecules, and condensed phases, is studied in physics, chemistry, and materials science using DFT, a computational quantum mechanical modelling technique.

Numerous physical and chemical properties, such as lattice constants, cohesive/adsorption energies, band structures, surface reactivity,

thermochemistry, rate constants, and others, can now be obtained with reasonable to high quality after decades of development, methodological advancements, and implementations. By creating interaction models of the different parts, it may probe the microscopic mechanism and pinpoint many essential parameters without jeopardizing the system's integrity. Experimental research has been greatly enhanced by advancement in computed methods enabling bold exploration into inaccessible domains DFT is currently a vital tool for modelling the properties of materials and molecules. Therefore, it also seems attractive to use DFT to predict NLO features. The first and second hyperpolarizability of POMs and their derivatives are being investigated by our team using DFT, which has been demonstrated to be an excellent method for analysing POM properties^{[38][50]}. The Results from the POM DFT study have shown improvements. in this work we have . investigated the stability, bonding type, and electrical properties of POMs using DFT.

Theoretical studies of NLO characteristics may support the development of new and interesting POM-based molecular NLO materials and validate the stated features of the POM system itself. in this thesis The NLO properties of hexamolybdate organoimido derivatives were predicted using DFT calculations, deconstructing how these POMs acquired their NLO features. Establishing a basis for a more thorough understanding of the NLO features of POMs is the aim of this work ^[89]. The last ten years have seen a large use of DFT to explain the energy and vibrational frequencies of D--A type molecules, as well as the structural properties of the ground and excited states. Theoretical studies of NLO

characteristics may help in the development of new and interesting POM-based molecular NLO materials as well as the validation of the stated features of the POM system itself.

In this thesis, it is predicted that the NLO properties of hexamolybdate organoimido derivatives using DFT simulations exhibit how these POMs acquired their NLO features. This work aims to establish a basis for a more thorough understanding of the NLO properties of POMs. The energy and vibrational frequencies of D- π -A type molecules, as well as the structural properties of the ground and excited states, have all been explained using DFT in the past ten years. Additionally, the computed values derived from this approach are accurate and useful for evaluating a variety of molecular properties.

Both the theoretical modelling of drug development and the quest for novel materials for photonics make use of the DFT^[47]. Several hexamolybdate complexes were calculated using DFT by our team, and the findings showed that the charge transfer from organoimido to hexamolybdate boosted the NLO responses of one-dimensional organoimido derivatives of hexamolybdate. However, by changing an organic ligand's length, the direction of charge transfer may be changed. Understanding the relationship between structure and properties with organoimido POM derivatives will be helpful in the creation of new NLO materials. The development of high-performance NLO materials may benefit from this effort.

2.9.1 Time-Dependent Density Functional Theory (TD-DFT):

The time-dependent extension of DFT (TD-DFT) allows to calculate and interpret optical absorption and emission spectra, which facilitates the investigation of charge-recombination and exciton transfer processes in organic electronic devices^[90]. In the earlier chapters, the mobility of coupled electrons was shown to be key factor in fluencing the discussed spectra.

When a powerful laser beam applied to an atom, molecule, or solid it reveals interesting non-perturbative phenomena arising from the complex electron

interactions. This phenomenon includes, for instance, non-sequential multiple ionization. These issues must be explicitly addressed by solving the (non-relativistic) time-dependent Schrödinger equation for the many-electron system.

(t) The ψ wavefunction:

$$\hat{H}(t)\psi(t) = i \frac{\partial \psi(t)}{\partial t}, \hat{H}(t) = \hat{T} + \hat{v}_{ee} + \hat{v}_{ext}(t) \dots \dots \dots (\text{Eq.2.17})$$

When $\hat{H}(t)$ is Hamiltonian Operator, Ψ is Wave Function,

\hat{T} is Kinetic Energy Operator, \hat{v}_{ee} is Electron-Electron Repulsion Operator, $\hat{v}_{ext}(t)$ is external potential, For a given initial wavefunction $\psi(0)$. Here the kinetic energy and electron-electron repulsion are expressed respectively:

$$\hat{T} = -\frac{1}{2} \sum_{i=1}^n \nabla_i^2 \text{ and } \hat{v}_{ee} = \frac{1}{2} \sum_{i=j}^n \frac{1}{|r_i - r_j|} \dots \dots \dots (\text{Eq. 2.18})$$

When: \hat{T} is Kinetic Energy Operator, ∇_i^2 is Laplacian Operator the external potential accounts for any field that is applied to the system (such as a laser) and the nuclear attraction:

$$\hat{v}_{ext}(t) = \sum_{i=1}^n v_i(r_i, t) \dots \dots \dots (\text{Eq.2.19})$$

When: $\hat{v}_{ext}(t)$ is external potential, The Coulomb interaction of electrons with a group of nuclei, for instance, can be represented by $v_{ext}(r_i, t)$, potentially following a classical route.

$$v_{ext}(r_i, t) = \sum_{v=1}^{N_n} \frac{Z_v}{|r - R_v(T)|} \dots \dots \dots (\text{Eq.2.20})$$

where Z and R_v represent the nucleus v 's charge and location, and N_n is the system's total number of nuclei (100). Despite the fact that hybrid TDDFT excitation energies for valence excitations are often excellent, the results are typically questioned in some challenging situations, such as Rydberg and charge transfer (CT) states or $\pi \rightarrow \pi^*$ excitations in conjugated systems

while certain hybrid functionals from specific families may predict these transitions with a reasonable level of accuracy, further study is required before their widespread application. Many ways were employed to improve the results for the ground- and excited-state characteristics. The two most popular theoretical

approaches are:^[91].

1. Range The separated (RS)
2. The DH, or double hybrid.

TDDFT balances accuracy and computational efficiency, making it one of the best techniques for studying electrical structure and optical excitations to date. Excitation energy, ionic force, and nonadiabatic coupling of excited states in solid- and molecular-state materials have all been calculated using linear-response TDDFT^[92].

2.9.2 ω B97XD:

To improve the potential overall accuracy of the Long -Range Corrected (LC) functionals, a methodical tuning strategy was recently used. With the same number of parameters, the LC form yields significantly improved results for all properties when the GGA exchange and correlation terms of the LC and hybrid functionals are modified. The ω B97XD Functional, which corresponds to an adjustable proportion of short-range exact exchange, is obtained by adding one more parameter to the whole functional optimization, which yields further statistically significant gains. The name of this LC functional is ω B97XD^[93]. These findings are supported by the following two different test sets: Unfortunately, because long-range correlation effects cannot be taken into account by semi-local correlation functionals, problems such as the lack of dispersion interactions (London force), which are associated with the lack of non-locality of the correlation hole, still persist^[94]. They were selected for this thesis since the long-range correlation impacts of the NLO effects for hexamolybdate organoimido compounds have already been evaluated and utilized by Rtib et al^[95].

2.10 Basis Sets:

The basis set selection is a crucial factor in any quantum computing. A basis in mathematics is an entire collection of linearly independent vectors that, when joined, may be used to represent any vector in that space. In Quantum physics,

basis functions are defined as a set of basic (often atomically inspired) functions that are used in linear combination to generate the entire electronic wavefunctions and/or electron density for a particular nuclear framework ^[49]. Whether for single point energy determination or geometry optimization, DFT calculations usually use a functional and a basis set to provide a finite mathematical representation of the atomic orbitals^[96]. The standard form of a basis function equation, where χ_s is the basis function and ϕ_i is the spatial orbital term, is shown in (Eq. 2.21). A collection of basis functions describing the spatial component of spin for a single electron on its own is called a basis set. Having these constant basis functions accessible for use in a functional makes solving Schrödinger's equation much easier. Over time, a number of foundation sets have been developed, each with a distinct degree of accuracy for the final result and appropriate for a certain purpose.^[83]

$$\phi = \sum_S C_{si} \chi_s \dots \dots \dots \text{(Eq.2.21)}$$

when: ϕ_i is the spatial orbital term,

Basis sets are divided into extended and minimum categories according to the quantity of basis functions included. By definition, an extended basis set provides more basis functions for the computation, allowing for the description of virtual orbitals or excited states, whereas minimal basis sets only contain basis functions that describe occupied orbitals within the designated chemical system. Though they frequently result in tenfold greater processing costs, extended basis sets can occasionally produce more accurate results" The less significant basis functions in your basis set may be better chosen with consideration Figure 2.3.

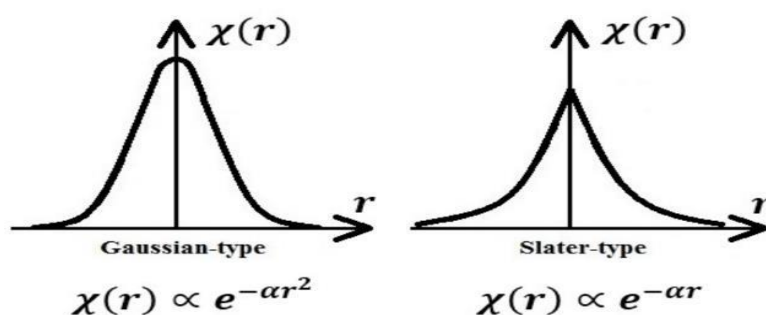


Figure 2.3 Slater and Gaussian functions for a 1s orbital. The Slater function is a good illustration of a hydrogen atom because of its sharp point at the apex. The photograph was taken by Moradabadi, A. ^[49].

displays two forms of basis functions: orbitals of the Slater (STO) and Gaussian (GTO) types. Despite providing a more accurate depiction of the hydrogen atom, STOs have the drawback of being more computationally expensive. Although GTOs are less precise than STOs, a particular technique that combines many GTOs linearly to create an overall function with a shape more similar to a STO. This approach enables basis the construction of function that is as accurate as a STO while reducing the amount of processing needed.

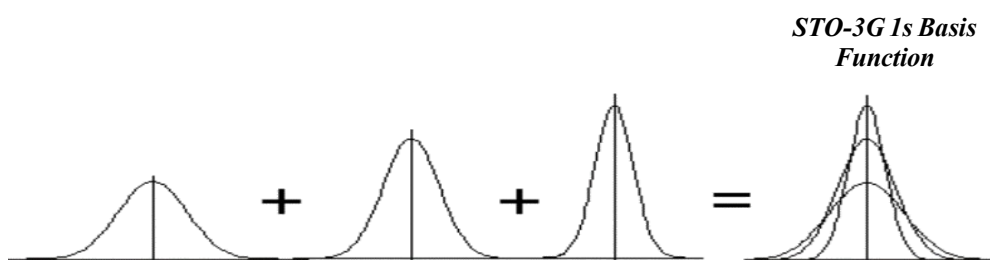


Figure 2.4 A pseudo-Slater function is produced by combining Gaussian-type functions ^[49]

The fact that GTOs are more efficient than STOs should come as no surprise, as all of the major DFT software programs use them, with ADF being the exception. Because there are so many affordable numerical integration algorithms available, STOs are still a good option for a basis function because they provide one with the freedom to use a variety of approaches to get convergence (AOs) more accurately than GTOs, but they still don't match the actual data.

Increasing the number of STOs inside a single basis function is a simple way to significantly improve the margin of accuracy. Since the orbital exponent (ζ_n) of each STO varies in this situation, the variational coefficient (C_n) has a "n" number of possible values. Coefficient selection is performed using computer software to determine the most appropriate exponent values that best represent the electron density for the molecular ground state at a given location; the charge density that is farther from the nucleus is described by the exponent with the smallest "n" value, and vice versa. Two STOs (D_i) and one polarization function per basis function (P) exist for the simplest STO basis set, DZP, as defined in (Eq. 2.22).

Polarization functions must be included in asymmetric AOs inside molecules; a polarization of an AO occurs if it is associated with another AO whose angular momentum quantum number is one value more than the original AO's. In systems that include a mix of metal and non-metal atoms bonded together inside a single molecule, polarization functions are consequently required.

$$R_{2s}(r) = C_1 e^{-\zeta_1 r} + C_2 e^{-\zeta_2 r} \dots \dots \dots \text{(Eq. 2.22)}$$

Incorporating extra polarization functions or STOs into the basis function may further complicate Karlsruhe basis sets. The TZP or QZP types of basis set are obtained by increasing the number of STOs by one or two functions. It is possible to expand ADF to include four polarization functions in total, recognized to be near the DFT level's complete basis set limit for molecules, which is the point at which a molecule cannot be represented with any greater level of accuracy. The most challenging basis set in the program is QZ4P. The computation time is increased by the number of core electrons and the inclusion of relativistic effects. Although contracting the Dirac-Fock equation can be complex, the use of Effective Core Potentials (ECPs), simplifies the problem. Even if the Dirac-Fock equation is difficult to construct, the fundamental concept behind ECP is to use it to calculate the all-electron wavefunction of an atom^{[97][98]}. The next step is to replace the core potential with a potential parameterized using

the appropriate set of analytical functions (either Gaussian Bessel functions or spherical functions). Next, the parameters of the original all-electron wavefunction are adjusted to match those of the approximation wavefunction.

The $(n + 1)$ s-, $(n + 1)$ p-, and (n) d-orbitals are usually the valence orbitals of transition metals, while the remaining orbitals are treated by (ECP). This group may be enlarged or contracted to include more (fewer) electrons, even if this approximation produces satisfactory results. Since there are a lot of heavy transition components in POMs, it is obvious that using ECP would enable quicker calculations. In the following sections, the innermost and valence electrons of POMs will be explained using the family of ECPs in conjunction with the Hay and Wadt basis set^[49].

2.10.1 LANL2TZ:

Many DFT calculations use LANL2DZ basis sets. However, the expected transition metal atomic state ordering shows how poorly the DF techniques can reproduce the experimental counterpart.

One of the most harmful consequences of this restriction is the energetics of reaction steps and the binding energy of systems, including transition metals.

The bulk of the statistics mentioned above may be accurately reproduced, though, by utilizing particular basis sets. The Stuttgart group provides double- or triple-zeta quality or greater size basis functions for a number of well-known effective core potential basis sets. The LANL2TZ basis sets, developed by Hay and Wadt at Los Alamos National Laboratory, are frequently employed in quantum chemistry research on molecules or clusters that include heavy elements^[99]. These basis functions were produced by using Gaussian functions to fit pseudo-orbitals^[100].

2.11 Inverse Design:

Modern society demands more time and resources to address major existential issues for human survival and well-being, therefore new approaches to

chemical discovery must be developed and used rather than relying solely on chance or raw force to advance science. These earlier approaches depend on the application of a novel material being obvious, which mostly depends on the researchers knowledge of where the material might be useful and one of the primary areas it the primary key of study within a certain time period ^[101]. Inverse design is a method that might provide an alternative while searching for novel, revolutionary materials.

Using this method, a molecule or material is designed by first developing a theoretical model of the product, one that is expected to have a particular function. Then, the synthetic route is worked backwards until the reagents and reaction conditions needed to produce the desired product are understood.

Additionally, inverse design provides a convenient to explore novel computational ideas, allowing researchers to assess the feasibility of idea before spending money on expensive laboratory work ^[102]. In other words, by identifying the optimal answer to a relevant research question rather than the other way around, inverse design can help researchers save a significant amount of lab time and money (Fig. 2.5).

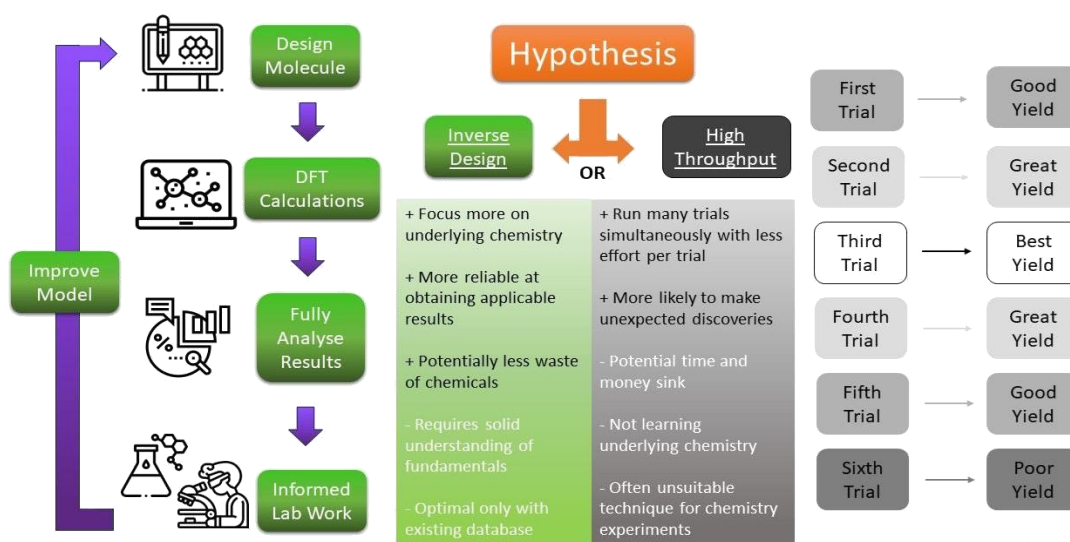


Figure 2.5. Diagram explaining differences between High Throughput and Inverse Design development methods. ^[103]

Working along with a machine learning software is obviously necessary to fully realize the promise of inverse design, which enables optimal solutions of an infinite number of alternative solutions. ^[103] Even though machine learning can be somewhat of a "black box," with only a small number of experts capable of comprehending and operating the program correctly, it remains a very fascinating field of study. Its strength lies in the ability to learn from the program's past experiences and adjust according to those experiences or new parameters. ^[101] The only computer program with the complexity and power required to sort through the plethora of options and find a chemical that is appropriate for the intended use is a machine learning program, which significantly shortens the development period. ^[104]

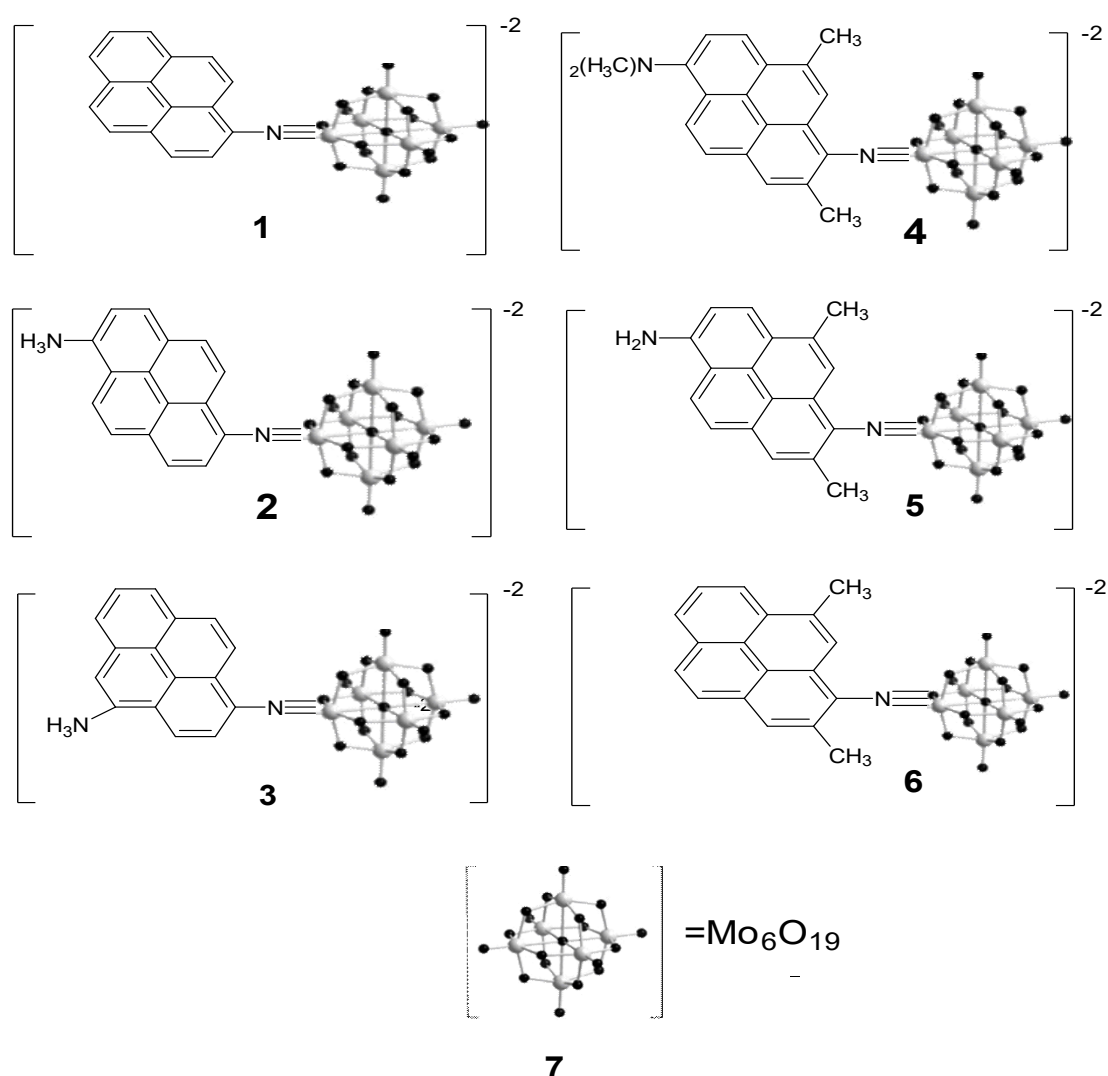
CHAPTER THREE

RESULTS AND

DISCUSSIONS

3.1 Results and Discussions:

This work aims to create novel organoimido hexamolybdates based on pyrene donors as NLO compounds. The development and study of a new class of organoimido Lindqvist derivatives using pyrene donor are presented in this chapter (scheme.3.1). This study represents the first reported application of DFT and TD-DFT analyses to investigate the electronic structure and linear/nonlinear optical properties of arylimido-POMs-pyrene derivatives.



Scheme 3.1 Molecular Structures of hexamolybdate-organoimido-pyrene compounds 1-6

3.2 Molecular Geometries in the Ground State for 1–6

Compounds:

Following geometry optimization of derivatives 1-6 at the SMD/ ω B97XD6-311+G(d)/LANL2TZ theoretical level, certain geometrical features for their ground-state geometries are displayed in Table 3.1. These geometries are compatible with known imido-species, including imido ($\text{Mo}\equiv\text{N}$) bonds with lengths ranging from 1.72 to 1.75 and imido angles on the $\text{Mo}=\text{N}-\text{C}$ axis between 171° to 177° . The form of derivatives 1 and 3 adopt geometries that are more compressed and curved.

Table 3.1 Selected Structural Constants For the Geometries of Compounds 1, 2, 3, 4, 5, and 6 with Distances in (Å) and Angles in ($^\circ$).

Compound	$\text{Mo}=\text{N}-\text{C}$	$\text{Mo}\equiv\text{N}$	N-C	$\text{Mo}-\text{O}^{\text{a}}\text{C}$	$\text{Mo}-\text{O}^{\text{b}}$
1	177.87	1.75	1.35	2.22	1.69
2	172.86	1.75	1.36	2.22	1.69
3	176.63	1.72	1.36	2.22	1.69
4	171.13	1.73	1.37	2.22	1.69
5	171.02	1.73	1.37	2.22	1.69
6	171.02	1.73	1.37	2.22	1.69

^a oxygen in the center. Mo-O length average in computed structures.

It was found that the value of the angle in the derivatives each of (4, 5 and 6) for $\text{Mo}=\text{N}-\text{O}$ is equal to 171.13° where as in derivatives (1 and 3), the angle increased to approximately (177°) this increase is due to the presence of such groups in the (Ortho) area for the amido group associated with pyrene, while in derivatives (1 and 3) the substituents are positioned at the meta sites. consequently, the ($\text{Mo}\equiv\text{N}$) is longer in derivatives 1 and 3 for (1.75) compound to those in (4, 5 and 6) which is equal to 1.73 [62].

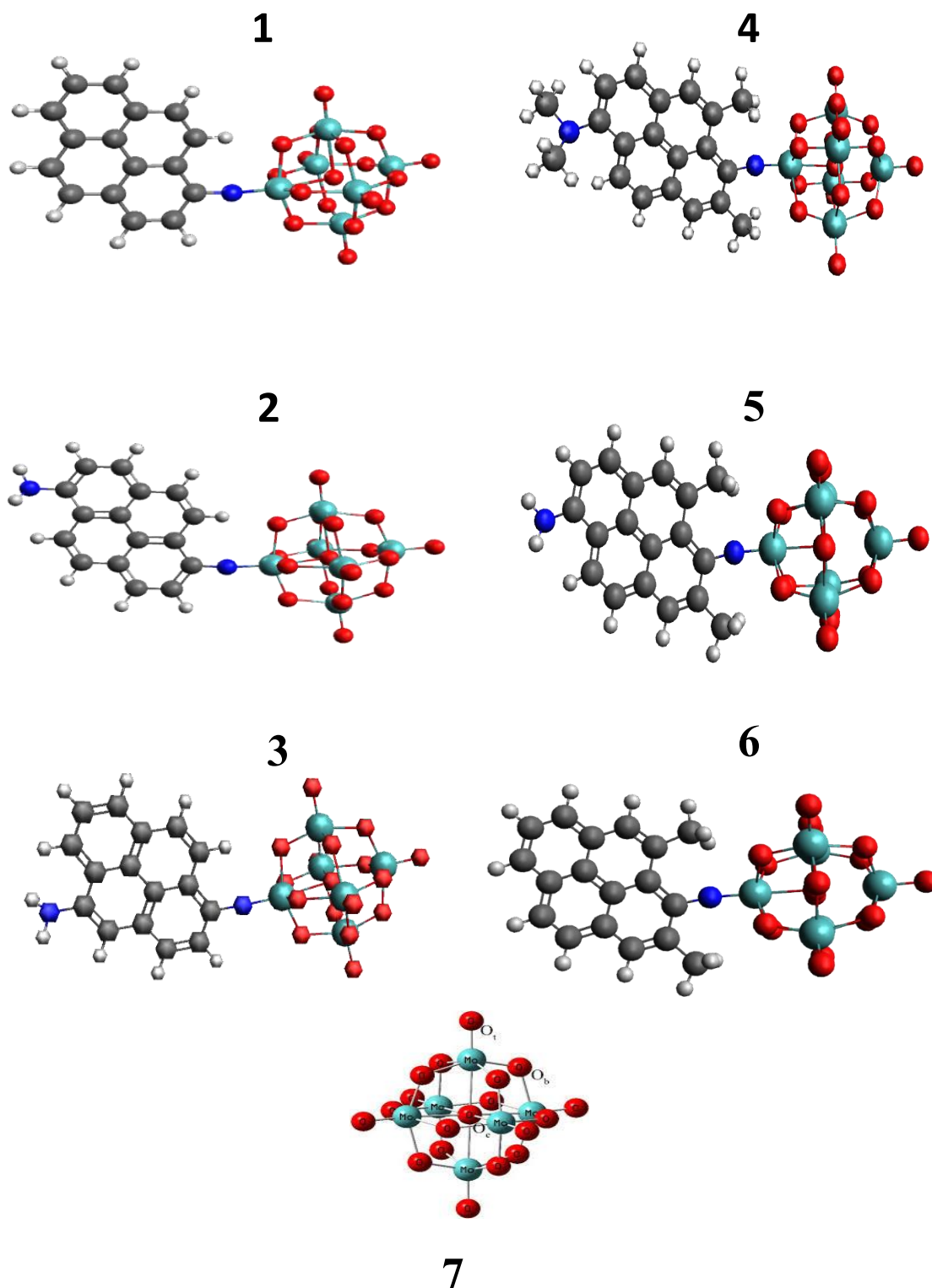


Figure 3.1 Solvent-Phase Optimized Geometries Of Anions 1–7.

Red = O, Blue = N, White = H, Cyan = Mo, and Gray = C.

3.3 Properties of NLO: Initial Hyperpolarizabilities For 1–6

Anions:

It is easy to compare the static and dynamic initial hyperpolarizabilities of compounds (1-6) at $\lambda = 1064$ nm and 1200nm, compared to available experimental data by using Table 3.2. The reference chemical, compound DAST,^[37] used at THz scanners at airports, has β_{zzz} and β_0 (25×10^{-30} esu) values that are much lower than those of the six compounds being studied, 1-6, theoretically. This indicates that the Pyrene donor group and the POM are communicating strong enough electronically, which leads to significant NLO activity. This could be attributed to the donor nature of the pyrene group which is stronger than other donors reported by previous studies. Anion 5 showed high values of β_{zzz} and $\beta_{zzz,0}$ at $\lambda_{\max} = 1064$ nm equal to (1349) and (397) respectively, while at $\lambda_{\max} = 1200$ nm equal to (655) and (397) respectively. The value of (γ_{zzz}) is the highest possible equal to (28121) at the $\lambda_{\max} = 1064$ nm unlike compounds (1-4, and 6) decreases in anions at $\lambda_{\max} = 1064$ nm. In contrast to anions 1 and 2, β_{zzz} and β_0 were seen to increase in anions 6 and 5, respectively, following methylation. Anion 5 showed beta-values of $\approx \times 2$ higher than its analogue anion 2. This could be due to the donating action of the methyl groups, which is supported by the analysis of the HOMO-LUMO energies that show a reduction in the energy of the aryl-based orbitals and somewhat boost the energies of the POM-based orbitals. Anion 2 showed the second largest NLO responses, both second-order and third-order.

Table 3.2 Calculated Initial Hyperpolarizabilities ($\times 10^{-30}$ esu) of Anions 1-6 compared with predicted and experimental Values For compound DAST

Calculated ($\times 10^{-30}$ esu)							
No.	$\lambda_{\max}(\text{nm})$	$\lambda = 1064 \text{ (nm)}$			$\lambda = 1200 \text{ (nm)}$		
		β_{zzz}	$\beta_{zzz,0}$	γ_{zzzz}	β_{zzz}	$\beta_{zzz,0}$	γ_{zzzz}
1	427	332	186	7309	238	186	4754
2	471	794	306	23821	483	306	11670
3	453	722	361	17232	484	361	9321
4	462	626	309	15119	432	309	9028
5	482	1349	397	28121	655	397	15813
6	434	373	201	8800	259	201	5426

3.4 The UV-Visible Absorption Spectra of Compounds 1–6:

UV-vis absorption characteristics were computed to understand orbital transition parameters associated with significant dipolar excited states. The lowest 100 transitions with a 50:50 mixture of singlet and triplet transition states were found using TD-DFT calculations in an acetonitrile solvent, (table 3.3). The table shows maximum absorption wavelengths (λ_{\max}) values (f_{os}), transition types, and oscillator strengths. For each anion studied, the low energy absorption band is formed from a single excited state with a non zero oscillator strength.

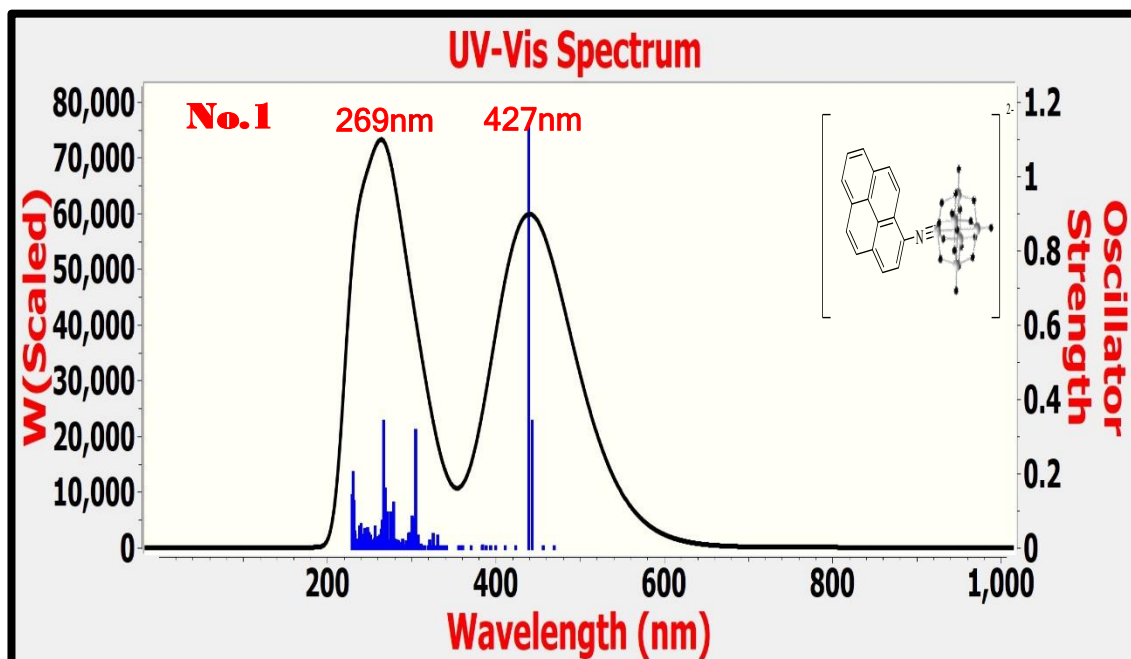
Comparing 1 and 2 and their ortho methylated counterparts, 6 and 5 respectively, reveals a modest increase in POM-based orbital energies and a slight decrease in compensated POM-based orbital energies leading to red-shift in the absorption spectrum.

Although, Anion 5 showed significant NLO responses, it maintained relatively high transparency. In contrast for anion 3 (ortho-amino pyrene), a slight blue splitting in all transition energies. This indicates less electronic resonance and communication between the pyrene (the donor) and POM part (the acceptor) which could be attributed to the sterically hindered molecular orbitals structure.

This is supported by the NLO results where anion 2 shows higher NLO responses than anion 3 (≈ 1.4 higher). In conclusion the ortho-amino pyrene-based organic derivatives have relatively less donor-character.

The All studied systems when compounded show relatively good transparency nonlinear windows compared to conventional organic chromophores of similar structures, as evidenced by slightly red-shift transitions in the maximum NLO responses. According to the HOMO/LUMO analysis, the HOMOs orbitals involved in the electronic transitions of all anions extend over the entire aryl imido unit with some POM character. While only POM affects the LUMO acceptor orbital of all anions. This clearly shows that the POM has significant charge-transfer involvement while acting as an acceptor during electronic transitions. Further evidence that the introduction of the strong donor pyrene in anions 2-5 is the reason for the rise in second order NLO activities stems from the formation of hybrid delocalized orbitals that extend from the pyrene to the POM group as wells from the expansion of the charge-transition. The orbitals of the imido group, and the bridge orbitals play a key role in the distinctive characteristics of the LUMO+ x acceptor orbitals. These findings indicate that POM participates in electronic transitions as an electron acceptor, there by resulting in significant NLO properties. Also, the formation of delocalized hybrid orbitals extending from pyrene to the POM group (CT extension) suggests that the incorporating the strong pyrene done enhances the increased activities of the second-order NLO. Figure 3.3 shows the molecular orbitals of anions 1-6 involved in significant transitions of HOMOs and LUMOs.

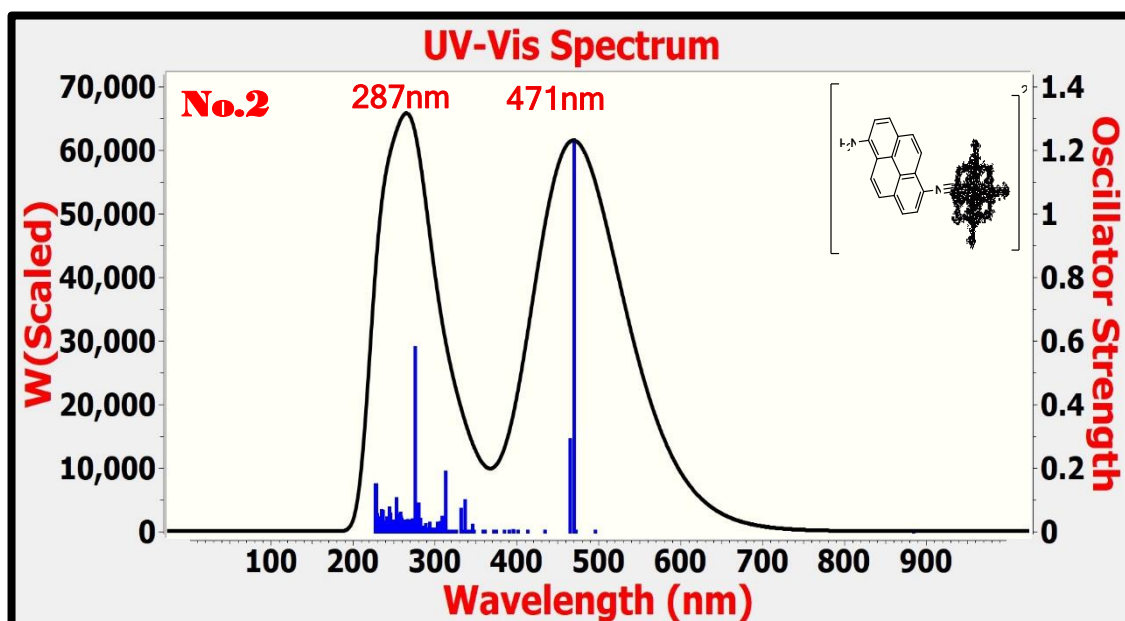
Calculated UV-Vis Spectrum:



Excited State **5**: Singlet-A Wavelength = 427nm, Oscillator Strength = 1.4825

Excited State **112**: Singlet-A Wavelength = 269nm, Oscillator Strength = 0.1997

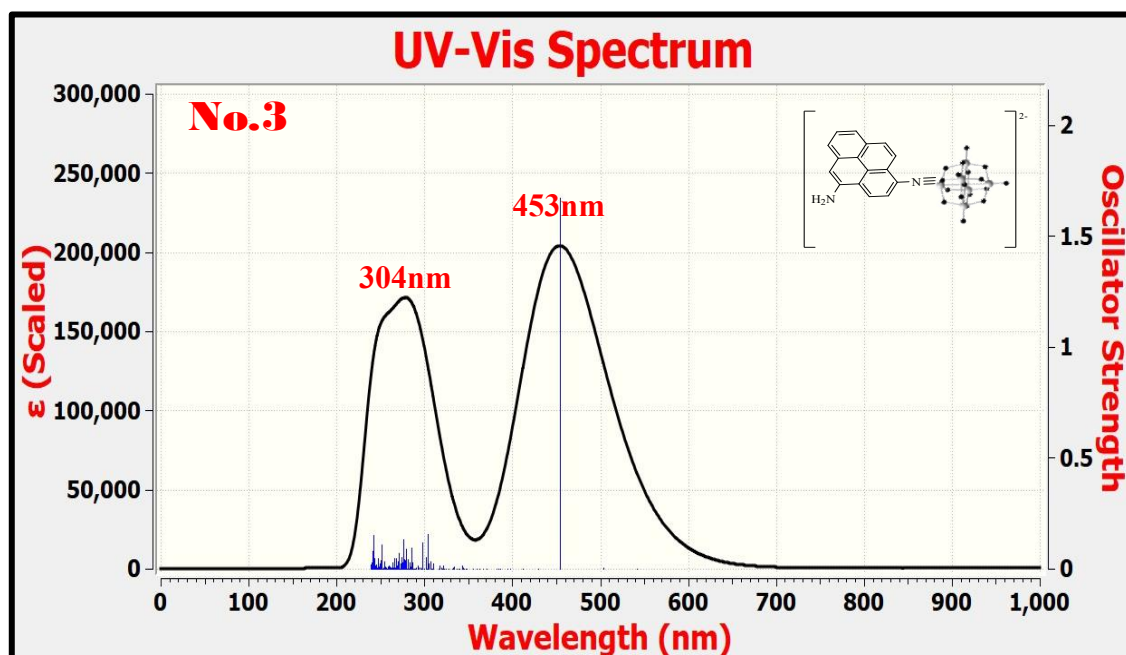
Calculated UV-Vis Spectrum:



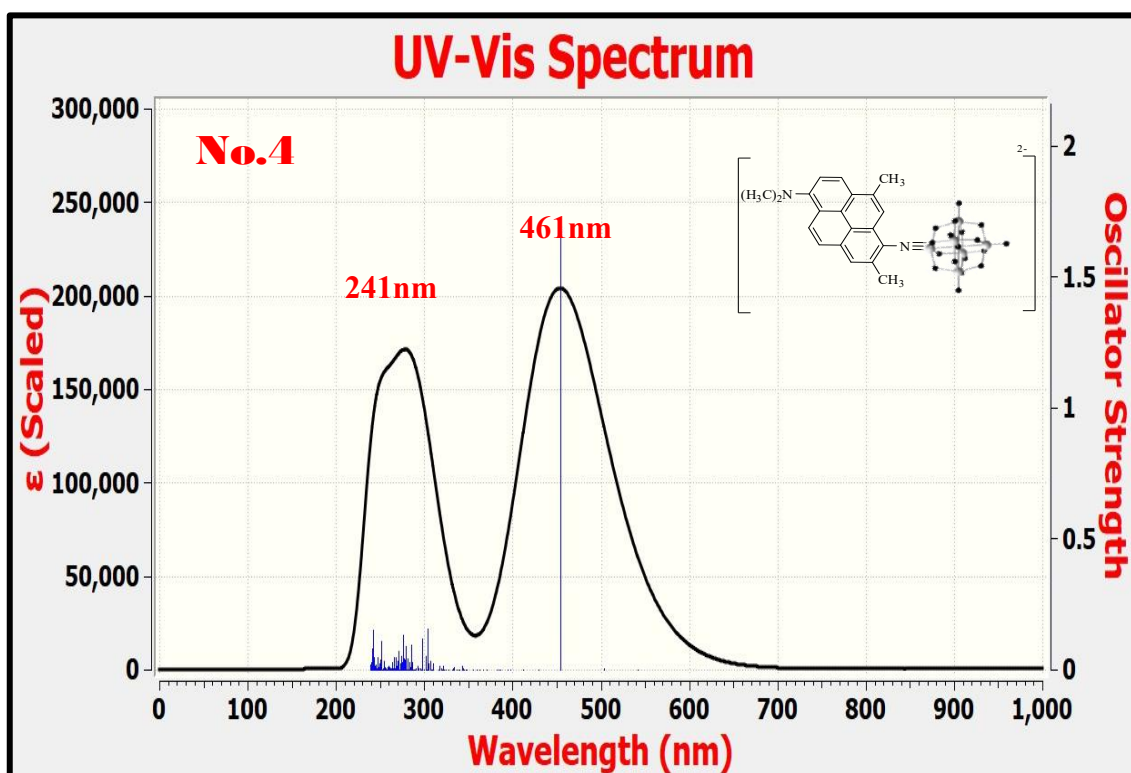
Excited State **4**: Singlet-A Wavelength = 471nm Oscillator Strength = 1.2312

Excited State **81**: Singlet-A Wavelength = 287nm Oscillator Strength = 0.5769

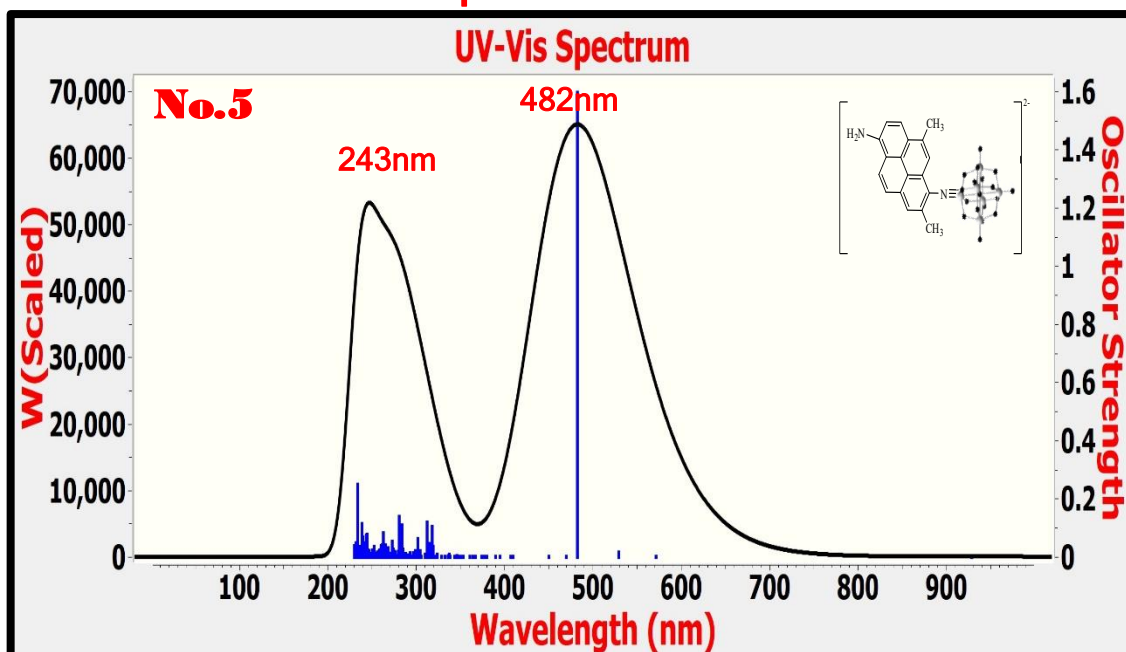
Calculated UV-Vis Spectrum:



Calculated UV-Vis Spectrum:



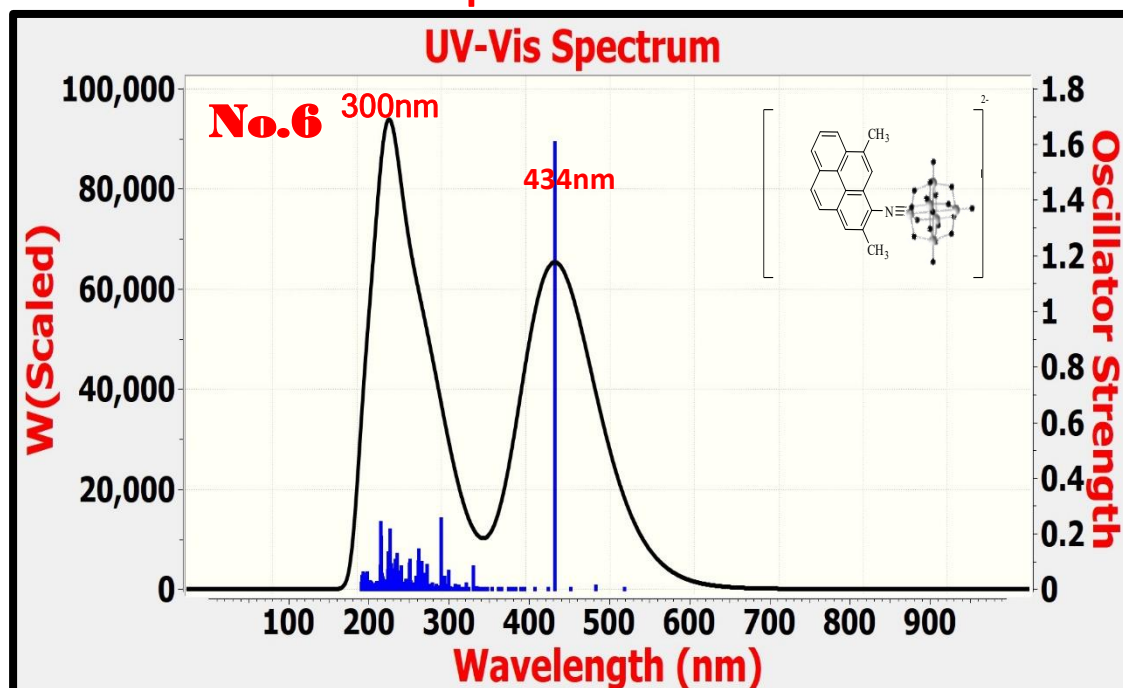
Calculated UV-Vis Spectrum:



Excited State **4**: Singlet-A Wavelength = **482nm**, Oscillator Strength = **1.5940**

Excited State **193**: Singlet-A Wavelength = **243nm** Oscillator Strength = **0.2484**

Calculated UV-Vis Spectrum:



Excited State **5**: Singlet-A Wavelength = **434nm**, Oscillator Strength = **1.6037**

Excited State **57**: Singlet-A Wavelength = **300nm**, Oscillator Strength = **0.2514**

Figure 3.2: TD-DFT-Calculated UV-Vis Spectra for No. (1, 2, 3, 4,5 and 6) Accordingly.

Table 3.3 The Electronic Transition Energy (E_{\max}), Oscillator Strength (f_{os}), Maximum Absorption Wavelength (λ_{\max}), and the % Mo Contribution (CON%) Were Computed.

Anion	n	λ_{\max} , nm	E_{\max} ev	f_{os}	$\Delta\mu_{ge}$, D	$E_{\text{HOMO-LUMO}}$ gap ev	μ_{ge} , D	Transition	CON.%
1	5	427	2.898	1.4825	16.6	5.729	28.1	HOMO→ LUMO +1	36
								HOMO→ LUMO +2	6
								HOMO→ LUMO +3	40
								HOMO→ LUMO +8	5.8
2	4	471	2.6278	1.231	19.1	5.424	32.4	HOMO→ LUMO	3
								HOMO-1→ LUMO +1	65
								HOMO → LUMO +2	2
								HOMO → LUMO +3	4
								HOMO→ LUMO +4	10
3	5	453	2.7321	1.673	24.9	5.477	35.7	HOMO→ LUMO +1	14
								HOMO→ LUMO +2	11
								HOMO→ LUMO +3	51
								HOMO→ LUMO +4	4
								HOMO→ LUMO +6	3
								HOMO→ LUMO +8	7
4	5	461	2.6843	1.6594	25.2	5.379	38.4	HOMO-2→ LUMO +3	2
								HOMO→ LUMO +2	22
								HOMO→ LUMO +3	57
								HOMO→ LUMO +6	2
								HOMO→ LUMO +8	7
								HOMO-2→ LUMO +3	2
								HOMO-11→ LUMO +5	2
5	4	482	2.5673	1.594	25.3437	5.21	37.35	HOMO→LUMO+2	10
								HOMO→LUMO+3	68
								HOMO→LUMO+6	2.5
								HOMO→LUMO+8	7.9
6	5	434	2.8505	1.6037	22.96	5.673	25.044	HOMO→LUMO+1	4.8
								HOMO→LUMO+2	34
								HOMO→LUMO+3	43
								HOMO→LUMO+8	5.9

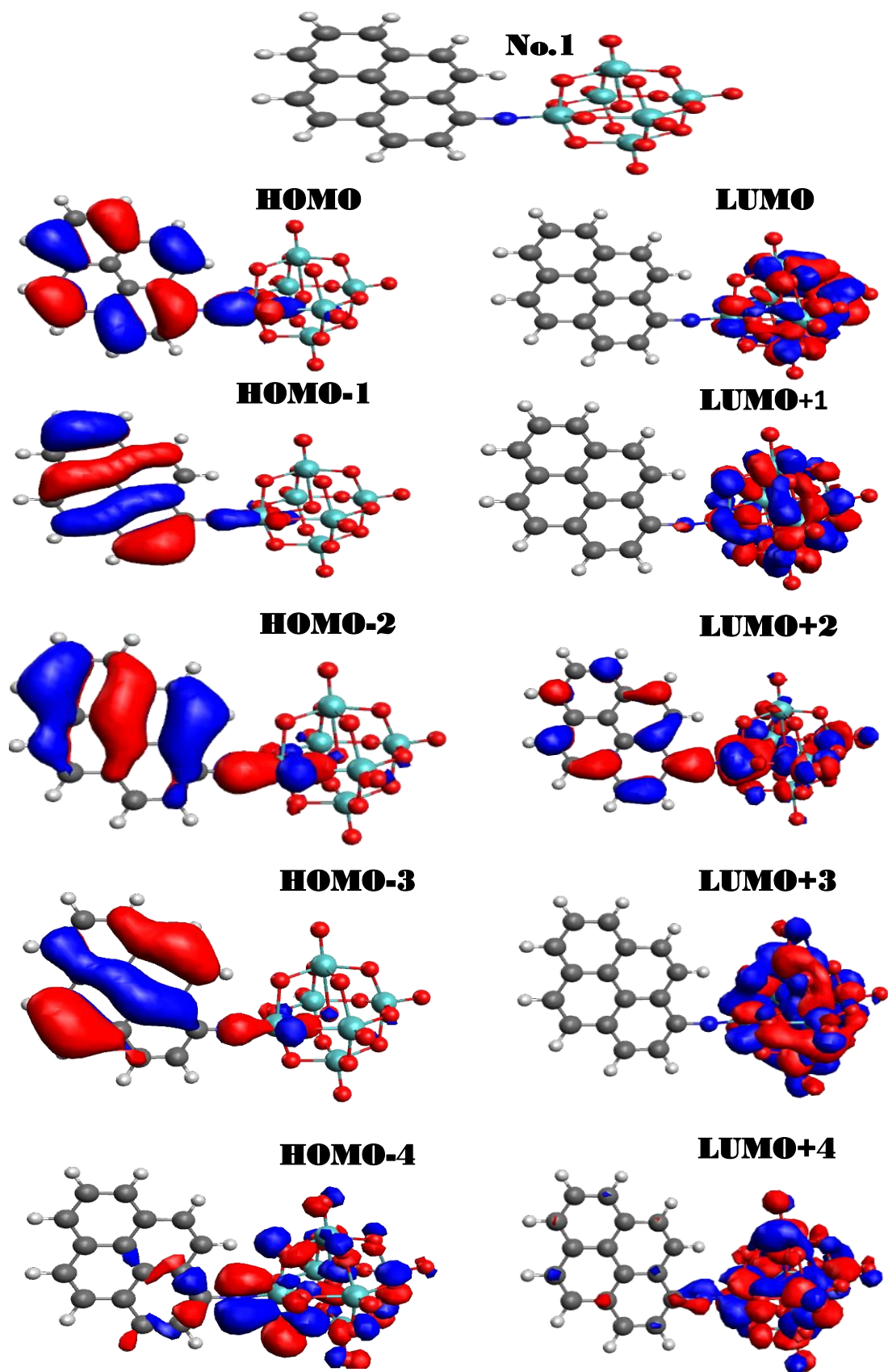


Figure 3.3 The Molecular Orbitals Involved In Significant Transitions of HOMO and LUMO No.1.

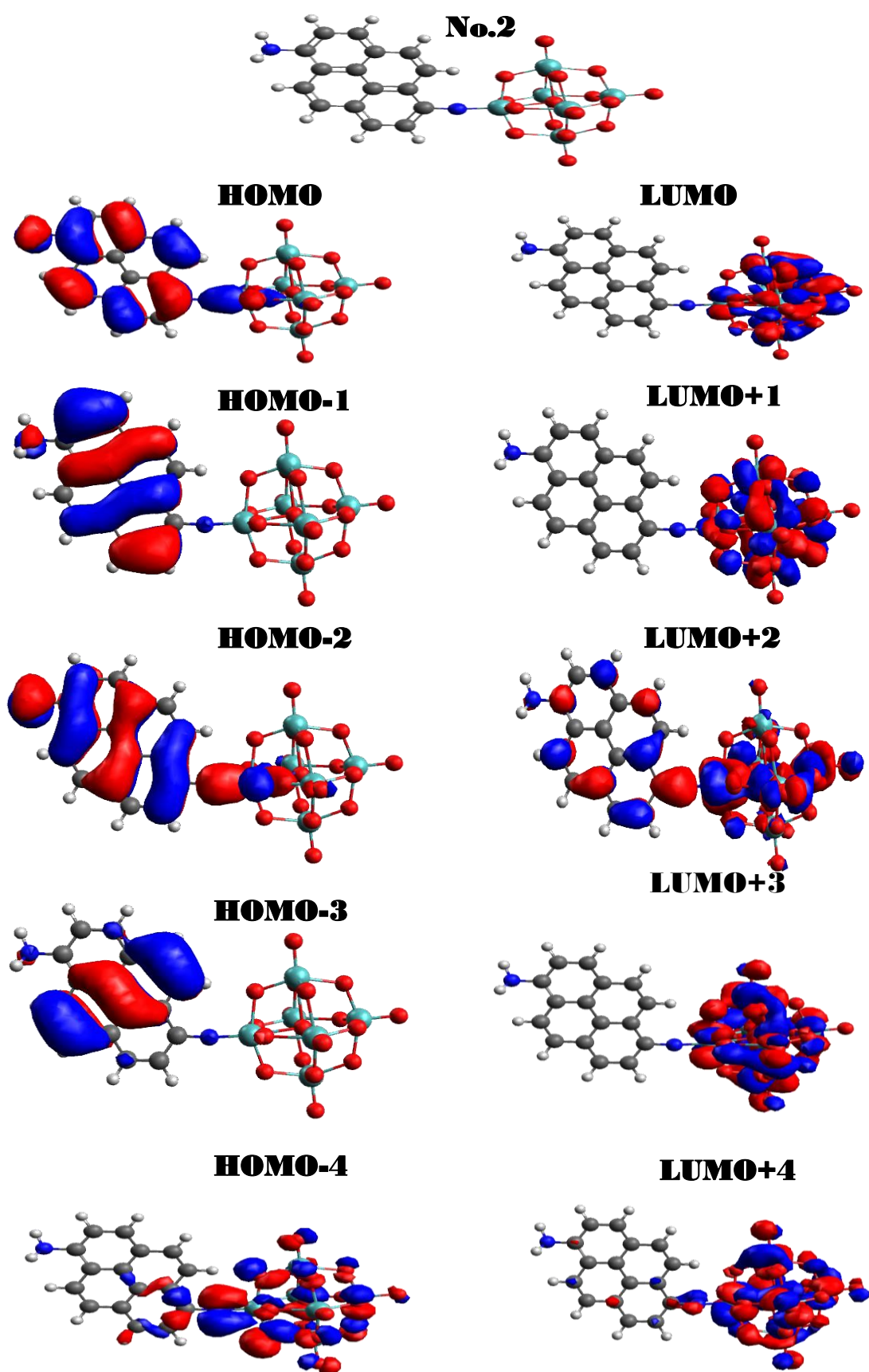


Figure 3.4 The Molecular Orbitals Involved In Significant Transitions of HOMO and LUMO No. 2.

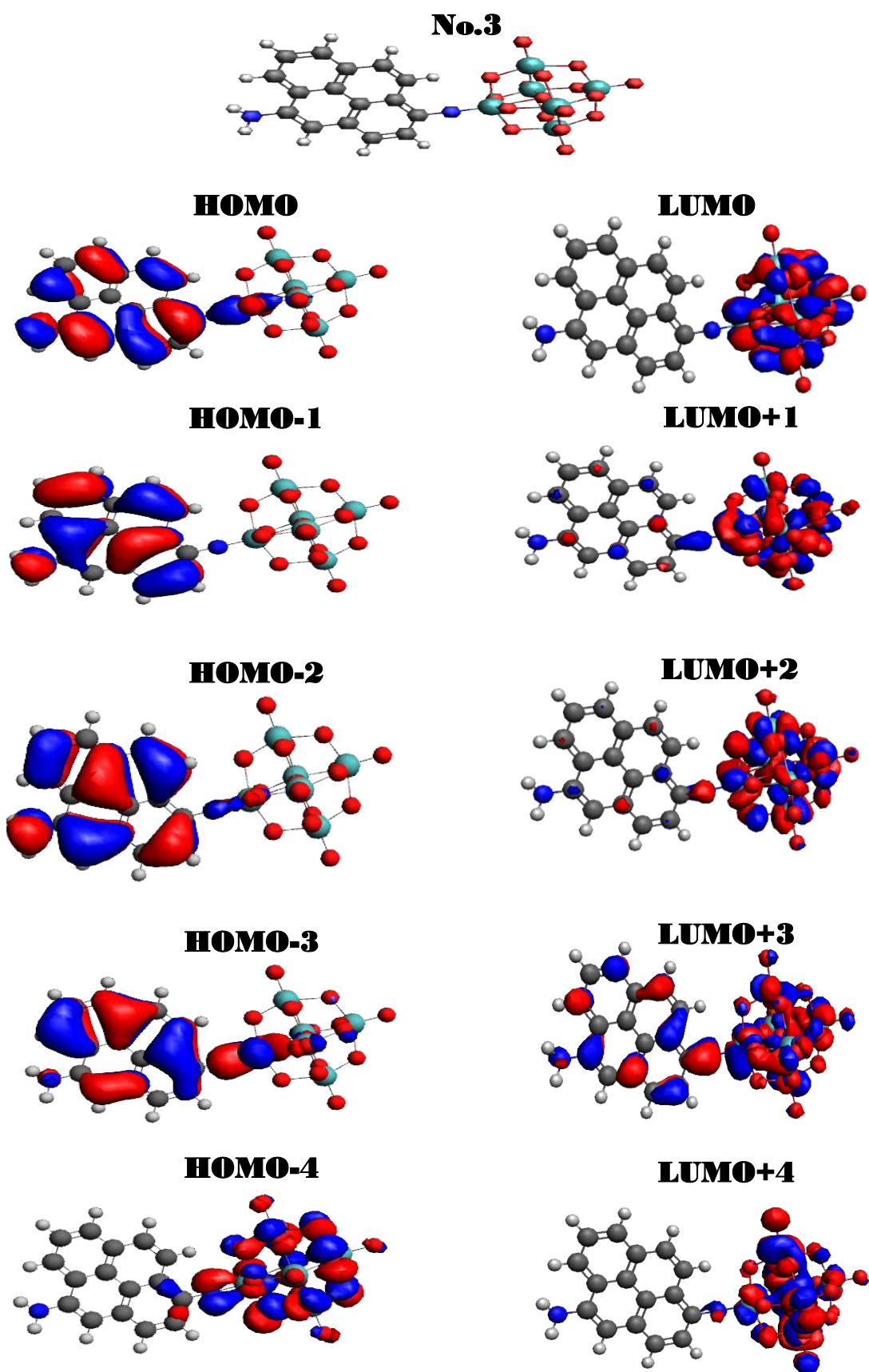


Figure 3.5 The Molecular Orbitals Involved In Significant Transitions of HOMO and LUMO No.3.

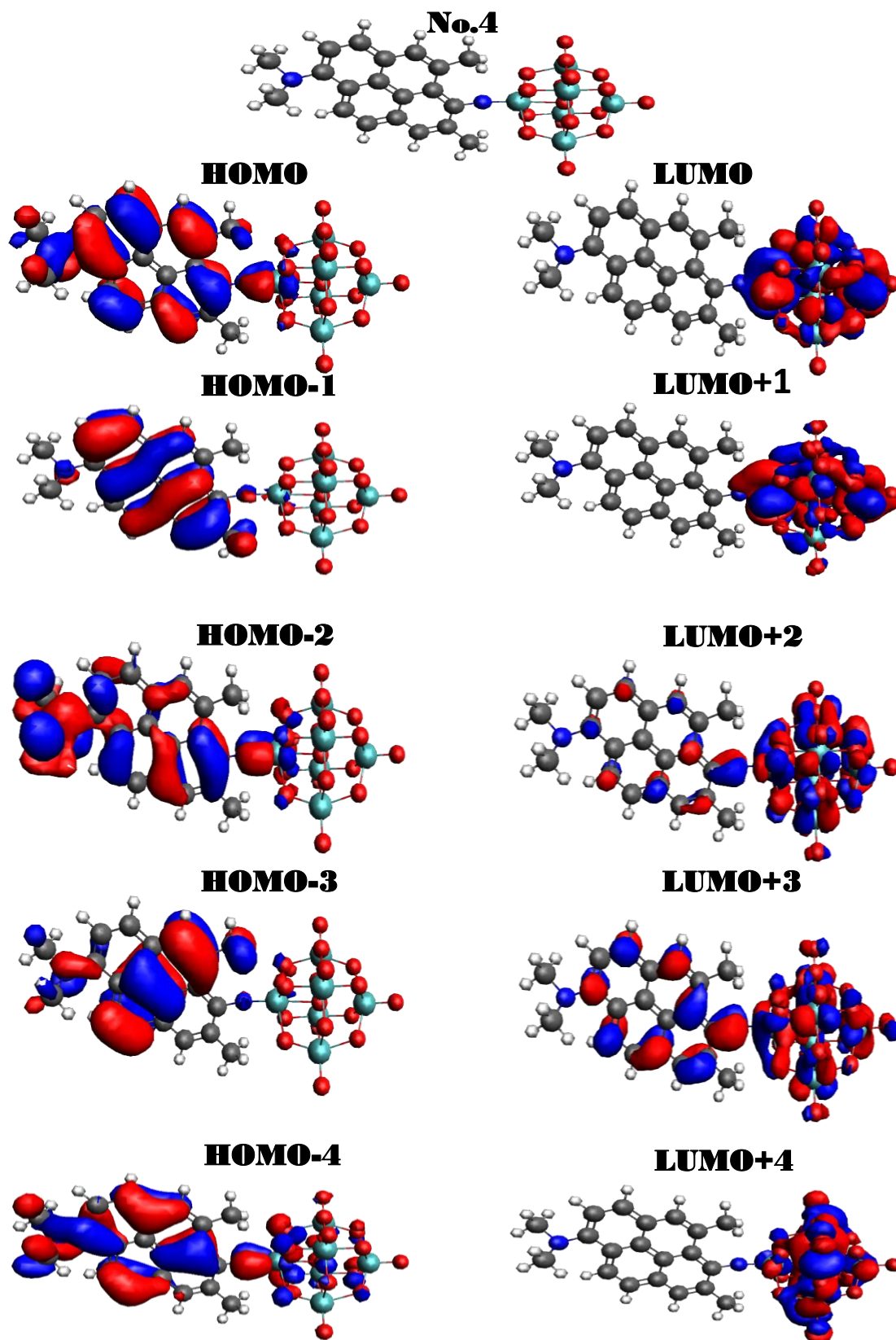


Figure 3.6 The Molecular Orbitals Involved in Significant Transitions of HOMO and LUMO No.4.

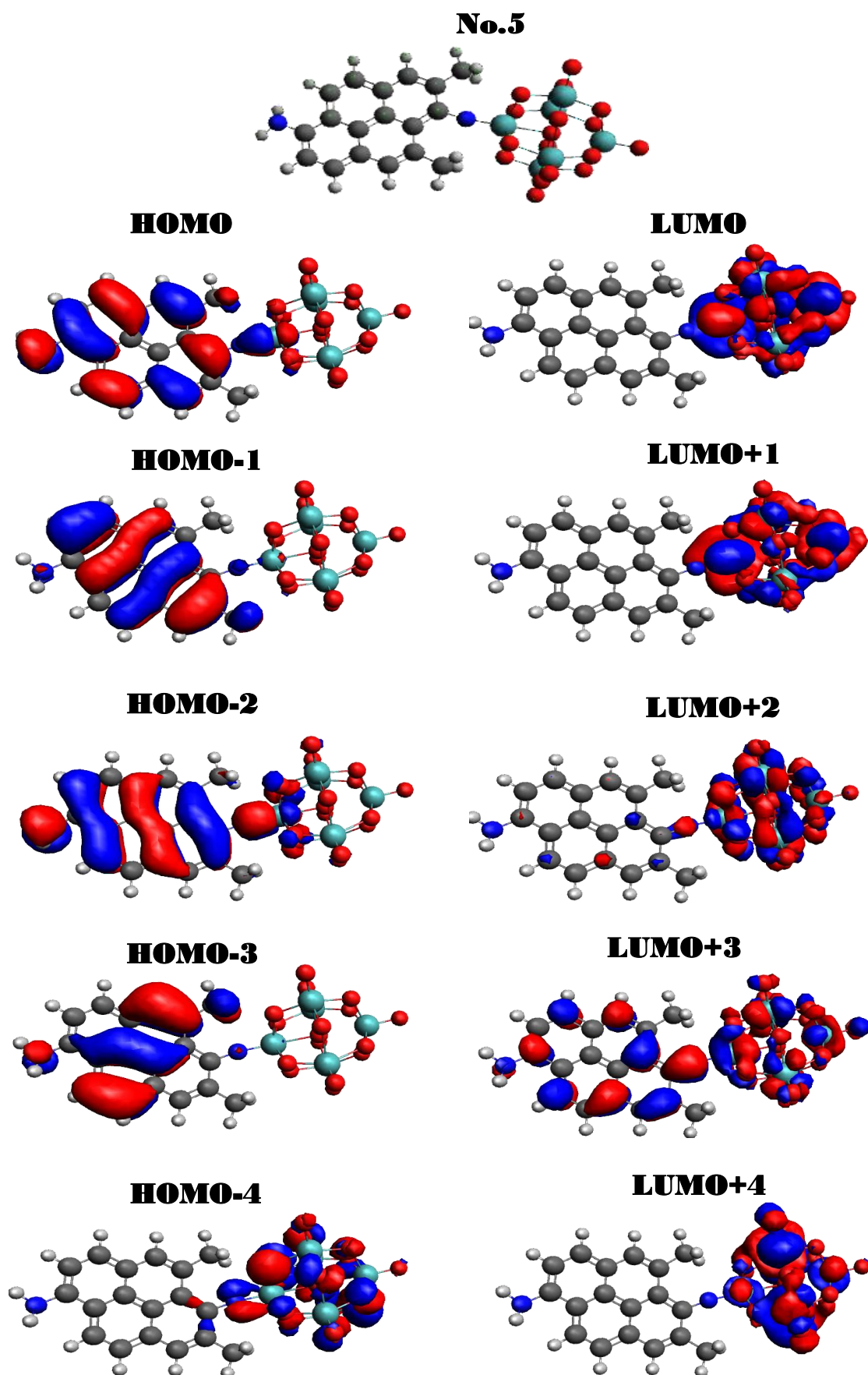


Figure 3.7 The Molecular Orbitals Involved In Significant Transitions of HOMO and LUMO No.5

According to Table 3.3, anion 5 has a higher $\Delta\mu_{ge}$ of 25.34 D with lowest $E_{\text{HOMO-LUMO}}$ gap among others indicating a higher degree of charge separation. This may be explained by the donation effect of the methyl groups, which reduces the energy of amido-based orbitals more significantly than POM-based orbitals. This observation is consistent with the shorter, and less curved, more linear imido-bond in anions 6 and 5.

3.5 Conclusion:

Using DFT/TD-DFT calculations, a novel class of Lindqvist-type hexamolybdate organoimido POMs derivatized with pyrene donor groups has been studied for second-order NLO application. The results demonstrate a significant improvement in the early hyperpolarizabilities while virtually maintaining the same transparency window, which might be explained by the donor strength of pyrene. Unit the significant excitation-induced electron transfer and dipole moment changes from the pyrene to the hexamolybdate core were responsible for the increased second-order NLO activity. Although the decrease in the first hyperpolarizability, ortho-methylation of the imido-bond has a major impact on bond stability, which in turn influences both bond length and homogeneity.

3.6 Future Projects:

The enhanced NLO properties in pyrene-POM materials is demonstrated by this work, and potential future research might involve the following:

1. Researchers may be inspired by the findings to synthesize these materials and look into their NLO properties.
2. Variation in pyrene substituents has the potential to influence NLO activity.
3. The effect of acceptor strength on the NLO per for Mance should be further examined by changing the POM types (Keggin, Anderson, etc.).

REFERENCES

REFERENCES:

- [1] Aithal S, Aithal P, ABJ of B&, **2024** undefined. Advancements in Nonlinear Optical Materials: Paving the Way for Future Photonic Devices [Internet]. Vol. 1, Poornaprajnapublication.Com. **2024**. Available from: <http://poornaprajnapublication.com/index.php/pijbas/article/view/17>
- [2] Waheed Zaman Khan, Roomana Yasmin, Hussain Akbar, Muhammad Irfan, Ghulam Mujtaba Noor, Hassan Ali, et al. Advancements in Laser Technology: Bridging Historical Milestones and Modern Applications in Science, Industry, and Sustainability. *Glob Sci Acad Res J Multidiscip Stud.* **2025**;4(1):70–84.
- [3] Qayyum H, Mamdouh S, Mahmoud A, Mohamed T. Nonlinear Optical Properties of Silver Nanoparticles: A Comprehensive Review. Available from: <https://lira.journals.ekb.eg/>
- [4] Wang H, Chen L, Wu Y, Li S, Zhu G, Liao W, et al. Advancing inorganic electro-optical materials for 5 G communications: from fundamental mechanisms to future perspectives. *Light Sci Appl* [Internet]. **2025**;14(1). Available from: <http://dx.doi.org/10.1038/s41377-025-01851-9>
- [5] Sanyasi Sitha. Effects of Various Bridges on Linear and Nonlinear Optical Properties of Some Push-Pull Type of Organic Molecules Department of Chemical Sciences Faculty of Science University of Johannesburg. **2017**;0002(August).
- [6] You JW, Panoiu NC. Nonlinear optical properties of 2D materials. *Encycl Nanomater.* **2023**;V1-562-V1-599.
- [7] Konforty N, Cohen MI, Segal O, Plotnik Y, Shalaev VM, Segev M. Second harmonic generation and nonlinear frequency conversion in photonic time-crystals. *Light Sci Appl* [Internet]. **2025**;14(1). Available from: <http://dx.doi.org/10.1038/s41377-025-01788-z>
- [8] Al-Yasari A. Synthesis, non-linear optical and electrochemical properties of novel

organoimido polyoxometalate derivatives. **2016**;221. Available from:

<https://ueaeprints.uea.ac.uk/id/eprint/59254/>

- [9] Fu S. Tailoring femtosecond laser filamentation in the atmosphere To cite this version :
HAL Id : tel-04884687 Tailoring femtosecond laser filamentation in the atmosphere.
2025;
- [10] Farhoomand A, Sepehri Javan N, Kheirandish A. Analytical investigation of second harmonic generation in metal nanoparticle trimers using dipole approximation. *Commun Theor Phys.* **2025**;77(6).
- [11] Dok AR, Legat T, de Coene Y, van der Veen MA, Verbiest T, Van Cleuvenbergen S. Nonlinear optical probes of nucleation and crystal growth: recent progress and future prospects. *J Mater Chem C.* **2021**;9(35):11553–68.
- [12] Hardy M, Chu HOM. Laser wavelength selection in Raman spectroscopy. *Anal .* **2025**;
- [13] Hail CU, Michaeli L, Atwater HA. Enhancement and Wavefront Control of Third Harmonic Generation with a Local High-Q Metasurface. *2024 Conf Lasers Electro-Optics, CLEO 2024.* 2024;
- [14] Liang ZX, Zhao YY, Chen JT, Dong XZ, Jin F, Zheng ML, et al. Two-photon absorption under few-photon irradiation for optical nanoprining. *Nat Commun* [Internet]. **2025**;16(1):1–9. Available from: <http://dx.doi.org/10.1038/s41467-025-57390-9>
- [15] Fu W, Shi X, Shi L, Mohanraj SS, Gao Y, Qi L, et al. Passive All-Optical Nonlinear Neuron Activation via PPLN Nanophotonic Waveguides. **2025**;1–12. Available from: <http://arxiv.org/abs/2504.18145>
- [16] Ashraf Hussein Saleh Supervised by Asst Asst Ahmed Hadi Al-Yasari Hasan Fisal Alesary B. A study the Optical and Electrochemical Properties of Polyoxometalate-Based Non-Linear Optical Compounds. **2023**;
- [17] Moss D. Optical data transmission at ultrahigh speeds , beyond 40Tb / s , based on a

soliton crystal micro- comb chip source. :1–25.

- [18] Nithyananda Kumar RS, Martulli A, Lizin S, Deferme W. The research path to commercialization: A perspective on plasmonic nanoparticles in organic and perovskite optoelectronics. *Prog Mater Sci.* **2025**;153(August 2024).
- [19] Mohammed SS, Al-Mahmoodi H, Yalda MI. Selecting Suitable Reference Gene for RT-qPCR Normalization in FFPE Breast Cancer Tissues for Duhok/Iraqi Women. *Al-Nahrain J Sci.* **2024**;27(5):93–105.
- [20] Kurniasih A, Previana CN. Implementation of GridSearchCV to Find the Best Hyperparameter Combination for Classification Model Algorithm in Predicting Water Potability. **2025**;4(2).
- [21] Bonvicini A, Forbes KA, Andrews DL, Champagne B. Hyper-Rayleigh scattering optical activity: Theory, symmetry considerations, and quantum chemistry applications. *J Chem Phys [Internet].* **2023**;158(20). Available from: <https://doi.org/10.1063/5.0152784>
- [22] Pleijers RFE, Nijdam S, Limburg AAA, Guo Y, Bagheri B, González A, et al. A numerical and experimental investigation on the physics of E-FISH when using a focused Gaussian probing beam 3MA60 Master Graduation Project. **2021**;
- [23] García HT, Garcia HT. Design and Characterisation of Hybrid Organic-Inorganic Materials for Luminescence Downshifting Devices University of Cambridge Department of Materials Science and Metallurgy. **2024**;(July).
- [24] Speelman R, Marker EJ, Geiger FM. Quantifying Stern layer water alignment before and during the oxygen evolution reaction. *Sci Adv.* **2025**;11(10):eado8536.
- [25] Dolai J, Ray R, Ghosh S, Maity A, Jana NR. Optical Nanomaterials for Advanced Bioimaging Applications. *ACS Appl Opt Mater.* **2024**;2(1):1–14.
- [26] Park G, Jung WS, Ra CS. First hyperpolarizabilities of nonlinear optical compounds: Susceptibility in donor-acceptor stilbene analogs. *Bull Korean Chem Soc.*

2004;25(9):1427–9.

- [27] Jannat A, Talukder MMM, Li Z, Ou JZ. Recent Advances in Flexible and Wearable Gas Sensors Harnessing the Potential of 2D Materials. *Small Sci.* **2025**;2500025.
- [28] Haq S, Khalid M, Braga AAC, Alhokbany N, Chen K. Design and evaluation of indacenothenothiophene based functional materials for second and third order nonlinear optics properties via DFT approach. *Sci Rep.* **2025**;15(1):1–18.
- [29] Esmailpour S, Nikoofard H, Sargolzaei M. Hypoxanthine : A DFT Investigation of Tautomerism and Nonlinear Optical Behavior HX1 HX2 Scheme 1 . The Tautomer structures of the. **2025**;1(1):22–9.
- [30] Ravele T, Fuku XG, Kebede MA. Review of Organic-Inorganic Heterojunction Hybrid Solar Cells with Embedded Plasmonic Nanocrystals: Recent Advances and Future Perspectives. *Energy and Fuels.* **2025**;
- [31] Abou-Shady A, El-Araby H. A comprehensive analysis of the advantages and disadvantages of pulsed electric fields during soil electrokinetic remediation [Internet]. Vol. 22, *International Journal of Environmental Science and Technology.* Springer Berlin Heidelberg; **2024**. 3895–3925 p. Available from:
<https://doi.org/10.1007/s13762-024-05996-9>
- [32] Baldini F, Dholakia K, French P, Guntinas-Lichius O, Kohler A, Mäntele W, et al. Shining a Light on the Future of Biophotonics. *J Biophotonics.* **2025**;1–18.
- [33] Ban S, Yi H, Park J, Huang Y, Yu KJ, Yeo WH. Advances in Photonic Materials and Integrated Devices for Smart and Digital Healthcare: Bridging the Gap Between Materials and Systems. *Adv Mater.* **2025**;2416899.
- [34] Qiu Z, Bruzzese PC, Wang Z, Deng H, Leutzsch M, Farès C, et al. 3-Center-3-Electron σ -Adduct Enables Silyl Radical Transfer below the Minimum Barrier for Silyl Radical Formation. *J Am Chem Soc.* **2025**;
- [35] Zhao Y, Huo X, Du H, Lai X, Li Z, Zhang Z, et al. Moderating effect of instrumental

- activities of daily living on the relationship between loneliness and depression in people with cognitive frailty. *BMC Geriatr.* **2025**;25(1).
- [36] Al-Yasari A, Van Steerteghem N, Kearns H, El Moll H, Faulds K, Wright JA, et al. Acousto-optic modulation of gigawatt-scale laser pulses in ambient air. *Inorg Chem* [Internet]. **2024**;14(1):4326–35. Available from: <http://arxiv.org/abs/2409.10227>
- [37] Shafiq I, Khalid M, Jawaria R, Shafiq Z, Murtaza S, Braga AAC. Exploring the photovoltaic properties of naphthalene-1,5-diamine-based functionalized materials in aprotic polar medium: a combined experimental and DFT approach. *RSC Adv.* **2024**;14(45):33048–60.
- [38] Department of Electrical Engineering, Osaka University, 2-1 Yamadaoka, Suita, Osaka 565-0871, Japan MS received 23 October **1998**
- [39] Mohitkar AS, Dey N, Jayanty S, Shehzadi K, Ayub K, Mahmood T, et al. Acousto-optic modulation of gigawatt-scale laser pulses in ambient air. *RSC Adv* [Internet]. **2024**;14(1):1–11. Available from: <http://dx.doi.org/10.1039/D4CP02750G>
- [40] Tahir M, Aftab H, Shafiq I, Khalid M, Haq S, El-Kott AF, et al. Synthesis, characterization and NLO properties of 1,4-phenylenediamine-based Schiff bases: a combined theoretical and experimental approach. *RSC Adv.* **2024**;14(6):4221–9.
- [41] Li L, Duan H, Qian J. Review on the study of Nonlinear Optics of Iridium Metal Organic Complex. *J Mater Sci Chem Eng.* **2021**;09(02):24–42.
- [42] Shafiq I, Irshad I, Zahid R, Mahmood K, Ahmed S, Bullo S, et al. Exploration of promising key electronic and nonlinear optical properties of bifluorenylidene based chromophores: a TD-DFT/DFT approach. *Sci Rep.* **2025**;15(1):1–15.
- [43] Shi LF, Zahid A, Ren A, Ali MZ, Yue H, Imran MA, et al. The perspectives and trends of THz technology in material research for future communication - a comprehensive review. *Phys Scr.* **2023**;98(6):0–22.
- [44] Jeong DS, Thomas R, Katiyar RS, Scott JF, Kohlstedt H, Petraru A, et al. Emerging

- memories: Resistive switching mechanisms and current status. *Reports Prog Phys.* **2012**;75(7).
- [45] Fan Y, Pei Y, Hu D, Wu Y, Sun K, Chen L, et al. A Lifetime Nanosensor for In Vivo pH Quantitative Imaging and Monitoring. *Small.* **2025**;(April).
- [46] Khenkin M, Köbler H, Remec M, Roy R, Erdil U, Li J, et al. Light cycling as a key to understanding the outdoor behaviour of perovskite solar cells. *Energy Environ Sci.* **2023**;17(2):602–10.
- [47] Bano R, Asghar M, Ayub K, Mahmood T, Iqbal J, Tabassum S, et al. A Theoretical Perspective on Strategies for Modeling High Performance Nonlinear Optical Materials. *Front Mater.* **2021**;8(December):1–24.
- [48] Suresh S, Arivuoli D. Nanomaterials for nonlinear optical (NLO) applications: A review. *Rev Adv Mater Sci.* **2012**;30(3):243–53.
- [49] Yu Y, Liu H, Chen K, Wu J. Segmented electric field poling of Si₃N₄-polymer hybrid electro-optic waveguides. :1–6.
- [50] Nadeem S, Anwar A, Khan MU, Hassan AU, Alrashidi KA. Synergistic charge-transfer dynamics of novel pyridoquinazolindone-containing triphenylamine-based push-pull chromophores: from structural optimization to performance metrics in photovoltaic solar cells and static, dynamic, solvent-dependent nonlinear opt. *RSC Adv.* **2024**;14(44):32482–500.
- [51] Hood BR, de Coene Y, Jones CF, Lopez Poves I, Deveaux N, Halcovitch NR, et al. Synthesis and Optical and Nonlinear Optical Properties of Linear and Two-Dimensional Charge Transfer Chromophores Based on Polyoxometalates. *Inorg Chem.* **2024**;
- [52] Biz C, Fianchini M, Gracia J. Strongly Correlated Electrons in Catalysis: Focus on Quantum Exchange. *ACS Catal.* **2021**;11(22):14249–61.
- [53] DeepSeek-AI, Guo D, Yang D, Zhang H, Song J, Zhang R, et al. DeepSeek-R1:

- Incentivizing Reasoning Capability in LLMs via Reinforcement Learning. **2025**;500:1–22. Available from: <http://arxiv.org/abs/2501.12948>
- [54] Janeiro R De, Yan Dalton Rodrigues Machado Optical characterization and optimization of nano and 2D materials Yan Dalton Rodrigues Machado Optical characterization and optimization of nano and 2D materials. **2025**;(January).
- [55] Lebbie D, Izuagie T, Pascual-Borràs M, Kandasamy B, Wills C, Waddell PG, et al. Protonolysis and Condensation Reactions of Alkoxido-Substituted Lindqvist {MW5} and Keggin {MPW11} Polyoxometalates: Comparative Experimental and Modeling Studies. *Inorg Chem.* **2025**;
- [56] Zhang S, Wang Y, Wang H, Luo Y, Yang A, Ye J, et al. Convenient synthesis of phthalonitrile-containing mono-benzoxazines with exceptional thermal stability and improved curing activity. *J Appl Polym Sci.* **2024**;(October).
- [57] Methodology FH, Mohammadi F, Conceptualization Z, Duval S, Supervision BM, Amiri A, et al. *Journal Pre-proof.* **2020**;
- [58] Hood BR, de Coene Y, Jones CF, Deveaux N, Barber JM, Marshall CG, et al. Donor and Geometry Optimization: Fresh Perspectives for the Design of Polyoxometalate Charge Transfer Chromophores. *Inorg Chem [Internet].* **2025**; Available from: <https://pubs.acs.org/doi/10.1021/acs.inorgchem.5c00915>
- [59] *The_efficacy_and_safety_of_ins.PDF.* p. 50.
- [60] Huang Y, Zhang J, Hao J, Wei Y. A general and highly regioselective synthesis approach to multi-functionalized organoimido derivatives of Polyoxometalates. *Sci Rep [Internet].* **2016**;6(January):2–11. Available from: <http://dx.doi.org/10.1038/srep24759>
- [61] Veríssimo MIS, Evtuguin D V., Gomes MTSR. Polyoxometalate Functionalized Sensors: A Review. *Front Chem.* **2022**;10(March):1–32.
- [62] Jalil MK, Mohammed AI. Synthesis of Hybrid Organic-Inorganic Polyoxometalates-

- based Materials for Optoelectronic Applications. **2023**;
- [63] Mroz AM, Basford AR, Hastedt F, Jayasekera IS, Mosquera-lois I, Sedgwick R, et al. Chem Soc Rev Cross-disciplinary perspectives on the potential for artificial intelligence across chemistry. **2025**;
- [64] Baharfar M, Hillier AC, Mao G. Charge-Transfer Complexes: Fundamentals and Advances in Catalysis, Sensing, and Optoelectronic Applications. Adv Mater. **2024**;2406083.
- [65] Venkatasubramanian V. Celebrating the Birth Centenary of Quantum Mechanics : A Historical Perspective. **2025**;
- [66] Gangwal A, Ansari A, Ahmad I, Azad AK, Kumarasamy V, Subramaniyan V, et al. Generative artificial intelligence in drug discovery: basic framework, recent advances, challenges, and opportunities. Front Pharmacol. **2024**;15(February):1–26.
- [67] Al-masoodi KOK. Computational Study on Biomimetic Model Ruthenium and Iron Clusters for Reduction of N₂. **2020**;(2013).
- [68]. Cascella M, Bore SL, Eisenstein O. The fellowship of the Grignard: 21st century computational tools for hundred-year-old chemistry. Chem Sci. **2025**;
- [69] Adeshina MA, Kim H. Exploring the frontier: Nonlinear optics in low dimensional materials. Nanophotonics [Internet]. 2025;1–23. Available from: <https://doi.org/10.1515/nanoph-2024-0652>
- [70] Dennington RD, Keith TA, Millam J. GaussView 5 reference. Vol. 53, Journal of Chemical Information and Modeling. **2013**. 1689–1699 p.
- [71] Jillani M, Sapari S, Bakar SIA, Razak FIA. Computational Insights into Nonlinear Optical Properties of Azobenzene Derivatives: A DFT-QSPR Approach. Malaysian J Fundam Appl Sci. **2025**;21(2):1883–96.
- [72] Löffelsender S, Beaujean P, de Wergifosse M. Simplified quantum chemistry methods to evaluate non-linear optical properties of large systems. Wiley Interdiscip Rev

- Comput Mol Sci. **2024**;14(1).
- [73] Song X, Wang X, Liu W, Chen X, Li S, Islam MS, et al. Organic Photo-Responsive Piezoelectric Materials Based on Pyrene Molecules for Flexible Sensors. *Adv Electron Mater.* **2025**;2400933:1–9.
- [74] Khan MU, Fatima A, Nadeem S, Abbas F, Ahamad T. Impact of π -Linkers Modifications on Tuning Nonlinear Optical Amplitudes of Pyridoquinazolinone-Based Aromatic Dyes: A Rational Entry to Novel D- π -A NLO Materials. *Polycycl Aromat Compd [Internet]*. **2023**;0(0):1–31. Available from: <https://doi.org/10.1080/10406638.2023.2266093>
- [75] Taghavi I, Moridsadat M, Tofini A, Raza S, Jaeger NAF, Chrostowski L, et al. Polymer modulators in silicon photonics: Review and projections. *Nanophotonics.* **2022**;11(17):3855–71.
- [76] Gao J, Liu X, Liu Y, Yu L, Feng Y, Chen H, et al. Experimental and theoretical studies on pyrene-grafted polyoxometalate hybrid. *Dalt Trans.* **2012**;41(39):12185–91.
- [77] McArdle S, Endo S, Aspuru-Guzik A, Benjamin SC, Yuan X. Quantum computational chemistry. *Rev Mod Phys.* **2020**;92(1).
- [78] Colombo A, Dragonetti C, Fagnani F, Roberto D, Guerchais V, Roisnel T, et al. Multifunctional Organometallic Compounds: An Interesting Luminescent NLO-Active Alkynylplatinum (II) Complex. *Eur J Inorg Chem.* **2024**;202400478(Ii):1–7.
- [79] Passalidis S. To cite this version : Sorbonne Université Thèse Modélisation de processus multielectroniques au cours de collisions atomiques. **2022**;
- [80] Korchagina K, Balasubramani SG, Berreur J, Gerard EF, Johannissen LO, Green AP, et al. Directed Evolution's Selective Use of Quantum Tunneling in Designed Enzymes—A Combined Theoretical and Experimental Study. *J Phys Chem B.* **2025**;
- [81] Monteiro JMC, Drigo Filho E. Tunneling Times in an Asymmetric Harmonic Double-Well with Application to Electron Transfers in Biological Macromolecules. *ACS*

Omega. **2024**;

- [82] Eissa Me. Review Article Times New Roman Article Info : 2024;9(5):113–21.
- [83] Richer M, Kim TD, Ayers PW. Graphical Approach to Interpreting and Efficiently Evaluating Geminal Wavefunctions. *Int J Quantum Chem.* **2025**;125(1).
- [84] Consiglio G, Gorczyński A, Petralia S, Forte G. Charge transfer properties of novel linear carbon chain-based dyes. *J Mater Chem C.* **2023**;12(3):903–12.
- [85] Andrews SS. *Light and Waves.* **2023**.
- [86] Buccio D, Percacci R. Renormalization group flows between Gaussian fixed points. *J High Energy Phys.* **2022**;2022(10).
- [87] Iammarino D, Iammarino D. God is a Boltzmann Brane : Arriving at God via Physicalism God is a Boltzmann Brane : Arriving at God via Physicalism. **2025**;
- [88] Khan RU, Tonner-Zech R. Optimizing Computational Parameters for Nuclear Electronic Orbital Density Functional Theory: A Benchmark Study on Proton Affinities. *J Comput Chem.* **2025**;46(8).
- [89] Fleming GR, Scholes GD, Cheng YC. Quantum effects in biology. *Procedia Chem* [Internet]. 2011;3(1):38–57. Available from: <http://dx.doi.org/10.1016/j.proche.2011.08.011>
- [90] Ernst L, Song H, Kim D, Würthner F. Photoinduced stepwise charge hopping in π -stacked perylene bisimide donor–bridge–acceptor arrays. *Nat Chem* [Internet]. **2025**;17(May). Available from: <http://dx.doi.org/10.1038/s41557-025-01770-7>
- [91] Kussmann J, Lemke Y, Weinbrenner A, Ochsenfeld C. A Constraint-Based Orbital-Optimized Excited State Method (COOX). *J Chem Theory Comput.* **2024**;
- [92] Kim Y, Bertagna F, D'souza EM, Heyes DJ, Johannissen LO, Nery ET, et al. Quantum biology: An update and perspective. *Quantum Reports.* **2021**;3(1):80–126.
- [93] Dumon AS, Rzepa HS, Alamillo-Ferrer C, Bures J, Procter R, Sheppard TD, et al. A computational tool to accurately and quickly predict ^{19}F NMR chemical shifts of

- molecules with fluorine-carbon and fluorine-boron bonds. *Phys Chem Chem Phys*. **2022**;24(34):20409–25.
- [94] Rushton PP. Towards a non-local density functiona description of exchange and correlation. **2002**;191. Available from: <http://theses.dur.ac.uk/3746/>
- [95] Malcolm D (2024). Improving Accuracy of Polyoxometalate Computational Models A thesis submitted to the Univermistry. **2024**.
- [96] Baker M. <sc>C</sc> entral <sc>I</sc> ntelligence <sc>A</sc> gency. In: Haote Li1, 2, Sumon Sarkar1, 2, Wenxin Lu1, Patrick O. Loftus1, Tianyin Qiu1, Yu Shee1, Abbigayle E. Cuomo1, John-Paul Webster1, H. Ray Kelly3, Vidhyadhar Manee3 S, Sreekumar3, Frederic G. Buono3, Robert H. Crabtree1, Timothy R. Newhouse1, *, and Victor S. Batista1 *, 1Department, editors. *Encyclopedia of Bioterrorism Defense* [Internet]. Wiley; **2005**. Available from: <https://onlinelibrary.wiley.com/doi/10.1002/0471686786.ebd0024>
- [97] Floris PS, Zozoulenko I, Rurali R. Doping Efficiency of Poly (benzodifurandione) from First Principles. **2025**;0–3.
- [98] Sawicki I, Triglione V, Jana S, Śmiga S. An Analysis of Regularized Second-Order Energy Expressions in the Context of Post-HF and KS-DFT Calculations: What Do We Gain and What Do We Lose? *J Chem Theory Comput*. **2025**;
- [99] Sheean et al. 2013, Jones R. 基因的改变NIH Public Access. *Bone* [Internet]. **2014**;23(1):1–7. Available from: <https://www.ncbi.nlm.nih.gov/pmc/articles/PMC3624763/pdf/nihms412728.pdf>
- [100] Bursch M, Mewes J, Hansen A, Grimme S. Best-Practice DFT Protocols for Basic Molecular Computational Chemistry**. *Angew Chemie*. **2022**;134(42).
- [101] Vilà-Nadal L. POMzites: A roadmap for inverse design in metal oxide chemistry. *Int J Quantum Chem*. **2021**;121(5):1–8.
- [102] Förster A, Visscher L. Low-Order Scaling Quasiparticle Self-Consistent GW for

Molecules. *Front Chem.* **2021**;9(September):1–14.

- [103] Kim B, Lee S, Kim J. Inverse design of porous materials using artificial neural networks. *Sci Adv.* **2020**;6(1):1–7.
- [104] Boyd T, Mitchell SG, Miras HN, Long DL, Cronin L. Understanding and mapping the assembly of a family of trimeric polyoxometalates: Transition metal mediated Wells-Dawson (M18)- trimers. *Dalt Trans.* **2010**;39(28):6460–

الخلاصة

تتألف هذه الرسالة من ثلاثة أقسام. يتناول القسم الأول مقدمةً عن المواد البصرية غير الخطية (NLO) وتكوين التوليد التوافقي الثاني (SHG)، بالإضافة إلى شرحٍ لعلاقة المانح والمستقبل وكيفية استخدام الجسور في نموذج الحالة الثنائية لربطهما. كما يناقش القسم الثاني البولي أوكسوميتالات (POM) ومشتقاته، بالإضافة إلى البيرين، أقوى مانح معروف. أما القسم الثاني فيتناول معادلة شرودنجر، متضمنةً أربعة تقريبات رئيسية، وكيمياء الكم، وهارترى-فوك (HF)، بالإضافة إلى خوارزمية تحويل فوربيه ثنائي الطور (TDDFT) وخوارزمية تحويل فوربيه ثنائي الطور (DFT)، وغيرها من المواضيع ذات الصلة. وقد وُصفت جميع النتائج في الجزء الثالث. وتُستخدم المواد البصرية غير الخطية (NLO) لتغيير ضوء الليزر من خلال ظواهر من الدرجة الثانية، مثل إنتاج التوافقي الثاني (مضاعفة التردد) وتأثيرات من الدرجة الثالثة، مثل امتصاص الفوتونات المتعددة. تركز هذه الرسالة على مواد NLO التي تتضمن مجموعات فينيل-إميدو التي تربط مانحي الإلكترونات العضوية بمستقبلات إلكترون بولي أوكسوميتالات (POM). لقد بحثنا بدقة في مركبات جديدة كمواد كيميائية قوية لـ NLO، مثل مجموعات المانحين القائمة على البيرين، وهي مانحات قوية للغاية، نظريًا وبشكل رئيسي من خلال حسابات DFT. بالإضافة إلى ذلك، تم تقييم خصائصها البصرية الخطية، واستجاباتها غير الخطية من الدرجة الثانية، وبنيتها الهندسية والكهربائية. علاوة على ذلك، تم دراسة آثار الاستبدالات (مثل مجموعات الألكيل) على قوة مانح البيرين، وبالتالي على الاستجابات. أنتج الأنيون 5 استجابات NLO ملحوظة تصل إلى $[1349 * 10^{-30}]esu$ بزيادة قدرها ≈ 2 مقارنةً بنظيره غير الميثيلي (الأنيون 2). تشير حسابات TD-DFT إلى أن الانتقال القوي منخفض الطاقة ناتج بشكل رئيسي عن انتقال الشحنة (CT) من أريل أميد البيرين إلى مجموعة الهيكساموليبيدات. وفقًا لذلك، يُعزى السلوك البصري الخطي وغير الخطي للمركبات إلى التواصل القوي بين مكونات POM والبيرين. على الرغم من أن عملية أورثوميثيليشن لرابطة الإيميدو تُقلل بشكل كبير من قابلية الاستقطاب الفائق الأولية، إلا أن لها تأثيرًا كبيرًا على استقرار الرابطة، وبالتالي على طولها وخطيتها، بالإضافة إلى نشاط NLO. مع الحفاظ على شفافية عالية، تُظهر نتائج TDDFT أن مزيج البيرين-POM يُظهر نشاط NLO استثنائيًا مقارنةً بالأنظمة العضوية البسيطة المشابهة.



جامعة كربلاء

تصميم ودراسة مواد هجينة جديدة ككروموفورات ضوئية لا خطية

رسالة مقدمة الى مجلس كلية العلوم /جامعة كربلاء وهي جزء من متطلبات
نيل درجة الماجستير في علوم الكيمياء

كتبت بواسطة

خميس شلال غياض

بإشراف

أ.د احمد هادي اليساري
أ.م.د ثائر مهدي مدلول

محرم / ١٤٤٧ هـ

حزيران / ٢٠٢٥ م